Report No. BMI-1488

UC-25 Metallurgy and Ceramics
(TID-4500, 15th Ed.)

Contract No. W-7405-eng-92

PROGRESS ON THE DEVELOPMENT OF URANIUM CARBIDE-TYPE FUELS

Phase II Report on the
AEC Fuel-Cycle Program

Edited by

Frank A. Rough
Walston Chubb

Work done by

Alfred E. Austin
Burton C. Boesser
G. Gregory Chesmar
Walston Chubb
George W. Cunningham
Joseph M. Fackelmann
Ellis L. Foster
David G. Freas
John E. Gates
Ralph W. Getz
John P. Hager
Donald L. Keller
Donald E. Kizer
Edward O. Speidel

December 27, 1960

BATTELLE MEMORIAL INSTITUTE
505 King Avenue
Columbus 1, Ohio

DISCLAIMER

TABLE OF CONTENTS

PROGRESS ON THE DEVELOPMENT OF URANIUM CARBIDE-TYPE FUELS

Phase II Report on the AEC Fuel-Cycle Program

Edited by Frank A. Rough and Walston Chubb

This report covers 1-1/2 years of a 2-1/2-year program for the development of uranium monocarbide on the AEC Fuel-Cycle Development Program. The results achieved in the first 6 months of this program were reported in greater detail in BMI-1370 (August 21, 1959).

Investigations in the field of chemical synthesis have demonstrated the feasibility of preparing uranium monocarbide from uranium metal by reaction with methane. The product obtained is suitable for direct compaction and sintering into pellets.

Powder metallurgical techniques have been developed for cold pressing and sintering uranium carbide powders containing excess uranium metal to densities above 90 per cent of theoretical. Hot pressing has been employed to consolidate uranium carbide powders to densities of essentially 100 per cent of theoretical.

The skull arc-melting and casting process for uranium carbide has been developed to where it is possible to make a single casting weighing up to 5 kg or several smaller castings having the same total weight.

The strength and hardness of uranium carbides are relatively insensitive to composition in the range from 4.8 to 9.0 w/o carbon. The 7.0 w/o carbon alloy is slightly harder than the other alloys in the as-cast condition. When heat treated to produce the U_2C_3 structure, the 7.0 w/o carbon alloy has a hardness of about 1100 KHN as compared to about 700 and 500 KHN for UC and UC_2, respectively. The strength and integrity of uranium carbides are very adversely affected by exposure to moisture. Alloying with refractory carbides alleviates this problem. Alloys of uranium monocarbide with Mo_2C, NbC, VC, and ZrC show high strength and hardness plus improved resistance to corrosion in Santowax R at 350 C, and constitute a new and highly promising class of carbide fuel materials.

Uranium monocarbide is compatible with aluminum and magnesium up to about 600 C, with mild steel and copper up to about 900 C, with stainless steel, Inconel, and zirconium to near or slightly below 800 C, and with niobium, molybdenum, and tantalum to about 1200 C, depending upon the exact conditions.

The activation energy for self-diffusion of uranium in uranium monocarbide is 82 kcal per mole or essentially the same as the activation energy for interdiffusion of uranium and carbon (79 kcal per mole). The rate of interdiffusion is over 500 times faster than the rate of self-diffusion of uranium.

Irradiations of uranium monocarbide to burnups of 0.01 and 0.03 a/o of the uranium have produced data that suggest that elastic expansion of the lattice reaches its limit between these two exposures, and that the additional stress applied to the lattice by exposures to burnups of 0.03 a/o and greater is relieved by reduction of the crystallite size.

INTRODUCTION

Uranium monocarbide is 25 per cent more dense than UO_2 and has a thermal conductivity at least three times greater than than of UO_2. It has a melting point 1400 C above that of uranium metal, and it has an isotropic, cubic crystal structure as compared to the anisotropic, orthorhombic crystal structure of uranium metal. The above properties alone tend to make UC the preferred fuel for certain types of nuclear reactors, and the recent discoveries that UC can be cast like a metal[1-3] and can withstand neutron irradiations to burnups of at least 1.5 total a/o[4-6] have suggested that UC may replace uranium metal almost entirely as a fuel for nuclear power reactors. On the other hand, the carbide is 28 per cent less dense than uranium metal and is much less corrosion and oxidation resistant than UO_2.

Various aspects of uranium carbide technology are presently under study at Battelle. The research is sponsored by the Reactor Development Division of the U. S. Atomic Energy Commission as a portion of its efforts to develop uranium carbide under the Fuel-Cycle Development Program. The program is divided into three temporal periods and into five subjective divisions for purposes of administration and reporting. The three temporal periods consist of 6 months, 1 year, and 1 year in consecutive order. This report covers the research performed in the second period (12 months long), designated Phase II. The five subjective divisions or areas of research are:

(1) An investigation of reactions and techniques by which uranium carbide powders (or other solid forms) can be synthesized and consolidated into dense bodies without resorting to melting and casting procedures. This part of the program has been directed toward producing more economical uranium carbide powder for powder metallurgical studies than can be prepared by melting uranium metal and carbon together and crushing the product. The products of various reactions have been characterized by analytical techniques and by subjecting them to various consolidation procedures, including cold pressing and sintering, liquid-phase sintering, and hot pressing. The prime objectives of this part of the program have been completed, and, at this time, no further work in this area is contemplated during Phase III.

(2) Development of equipment and techniques for melting and casting of uranium carbide shapes of reproducible dimensions, soundness, and analysis. This part of the program has been primarily concerned with perfecting the skull arc-melting and casting process for preparing massive shapes of uranium carbide. No serious problems have been encountered in connection with the operation of the equipment or in connection with the casting operation. Problems have been encountered in connection with control of the composition of the castings, and to solve these problems, this part of the research program will continue into Phase III.

(3) Determination of the physical and mechanical and chemical properties of uranium carbides as influenced by composition and processing variables. This part of the program involves determination and evaluation of the room-temperature hardness, strength, density, resistivity,

(1) References at end.

corrosion resistance, and microstructure of uranium carbides as affected by impurities and alloy additions and by heat treatment. Preliminary evaluations of the compatibility of carbides with metals have also been undertaken. These studies will continue through Phase III with more emphasis on determination of engineering properties at elevated temperatures. It is expected that such properties as strength, hardness, thermal conductivity, thermal-expansion coefficient, specific heat, and resistivity will be determined as a function of temperature.

(4) Measurement of the rates of interdiffusion and self-diffusion of uranium and carbon in uranium carbides. These basic physical data are expected to contribute to the understanding of many of the other high-temperature processes which can occur in uranium carbide such as sintering, grain growth, creep, phase changes, precipitation processes, relief of residual or radiation-induced stresses, and diffusion of fission products. Studies of interdiffusion rates have been completed, and studies of the rates of self-diffusion of uranium in uranium monocarbide are nearly complete and should be finished early in Phase III of this program. No suitable experimental technique for determining the rate of self-diffusion of carbon in uranium carbide has been devised as yet.

(5) Studies of the processes and mechanisms leading to damage in uranium monocarbide as a result of reactor irradiation. This part of the program has been involved in and directed toward the measurement of changes in such physical properties as resistivity, lattice parameter, and density as a function of reactor exposure. Microstructural changes as observed by optical and electron microscopy are also of interest. Two of the six reactor irradiations planned on this program have been completed, and the major effort in these studies is planned during Phase III.

Details of the progress that has been made in these five areas of research during the past year (Phase II) are described in the following pages.

DEVELOPMENT OF ALTERNATE FABRICATION TECHNIQUES

Several types of uranium carbide powders and different methods of solid-phase fabrication of these powders were investigated in this portion of the program. Although the basic aim was to devise methods for economical preparation of uranium carbide components, the fundamental aspects of uranium carbide powder preparation and sintering behavior were also studied. Powder was prepared by: (1) carburizing uranium metal with methane or propane, (2) crushing commercial uranium carbide shot, sinter cake, or buttons, (3) reacting UO_2 and carbon, and (4) synthesizing uranium carbide by arc melting and crushing the resultant buttons. These powders were analyzed chemically and metallographically and classified as to particle size. Compacts of these powders were fabricated by cold pressing and sintering, hydrostatic hot pressing, and conventional hot pressing. Sintering of mixtures of uranium and carbon as well as the effect of alloying

additions on the sinterability of UC were also studied briefly. The alloying agents used were Mo_2C, NbC, and chromium.

Preparation of Uranium Carbide For Use in Sintering Studies

Uranium-Methane Reaction

The feasibility and kinetics of producing high-quality uranium monocarbide by reacting uranium metal with a gaseous mixture of hydrogen and methane were studied both thermodynamically and experimentally. It was thought that, by adjusting the hydrogen/methane ratio in a flowing gas mixture, the activity of the carbon in the gas stream could be made equal to or greater than the activity of carbon in UC but less than the activity of carbon in UC_2. Under these conditions, uranium metal might be converted to stoichiometric UC at the reacting temperature. The pertinent equilibria for the uranium-methane reactions are:

$$U(s) + CH_4(g) \rightleftharpoons UC(s) + 2H_2(g) \quad (1)$$

$$UC(s) + CH_4(g) \rightleftharpoons UC_2(s) + 2H_2(g) \quad (2)$$

$$CH_4(g) \rightleftharpoons C(s) + 2H_2(g) \; . \quad (3)$$

In order to calculate the activity of carbon in UC and UC_2, as expressed for Equations (1) and (2), a brief literature survey was conducted to find free-energy data for UC and UC_2. The data considered most reliable were those derived by Ward.[7] Using Ward's data and suitable free-energy data for methane[8], the standard free-energy change (ΔF°) was calculated for the equilibria in Equations (1), (2), and (3). Since $\Delta F^\circ = -RT \ln K$ and $K = (p_{H_2})^2/(p_{CH_4})$ the values of $\log_{10} (p_{H_2})^2/(p_{CH_4})$ were calculated for the equilibria. The data and the results of the above calculations are tabulated in Table 1. In the absence of free-energy data for U_2C_3, UC and UC_2 were assumed to be the only stable phases in the uranium-carbon system between 800 and 1200 K.

The results of the calculations are thermodynamically inconsistent. In going from the two-phase region U + UC to the two-phase region UC + UC_2, which must represent an increase in the activity of carbon in the condensed phases, the calculations shown in Table 1 indicate that there is an increase in the partial pressure of hydrogen in the gas mixture, corresponding to a decrease in the activity of carbon in the gas phase. The chemical potential of carbon must be the same in both the condensed and gaseous phases, and an increase in the carbon activity in one phase must be accompanied by a corresponding increase in the other phase. Since calculations based on the free-energy data show the reverse situation to occur, the data must be in error. Another way of demonstrating this point is to examine the following equilibrium:

$$2UC \rightleftharpoons UC_2 + U \; . \quad (4)$$

Since ΔF° for this reaction at 1000 K, 727 C, would be -4,040 cal per mole using the data in Table 1, these data tell us that UC will decompose to form UC_2 and uranium at equilibrium at 727 C. Experimental data, as expressed in the uranium-carbon phase diagram, show that this situation is impossible.

TABLE 1. FREE-ENERGY AND LOG$_{10}$ $(P_{H_2})^2/(P_{CH_4})$ CALCULATIONS BASED ON THE DATA OF WARD[7] AND ROSSINI[8]

	800 K	900 K	1000 K	1100 K	1200 K
			ΔF^o, cal per mole		
$CH_4(g)$	-550	+2,010	+4,610	+7,220	+9,850
$UC(s)$	-18,495	-18,290	-18,010	-17,620	-17,170
$UC_2(s)$	-41,080	-40,636	-40,060	-39,330	-38,490
			ΔF^o, cal per mole		
$U(s) + CH_4(g) \rightleftharpoons UC(s) + 2H_2(g)$	-17,945	-20,300	-22,620	-24,840	-27,020
$UC(s) + CH_4(g) \rightleftharpoons UC_2(s) + 2H_2(g)$	-22,035	-24,356	-26,660	-28,930	-31,170
$CH_4(g) \rightleftharpoons C(s) + 2H_2(g)$	+550	-2,010	-4,610	-7,220	-9,850
			$\text{Log}_{10}(P_{H_2})^2/(P_{CH_4})$		
$U(s) + CH_4(g) \rightleftharpoons UC(s) + 2H_2(g)$	4.902	4.929	4.943	4.935	4.921
$UC(s) + CH_4(g) \rightleftharpoons UC_2(s) + 2H_2(g)$	6.019	5.914	5.826	5.747	5.676
$CH_4(g) \rightleftharpoons C(s) + 2H_2(g)$	-1.850	+0.488	1.007	1.434	1.794

Despite the inaccuracies in the available free-energy data, reasonable assumptions made it possible to approximate the equilibrium hydrogen/methane ratio over stoichiometric UC. It was thus determined from these data that at 1200 K, 927 C, where the gas-composition range is widest and the greatest opportunity for process control exists, the CH_4 composition limits for stoichiometric UC ranged from 0.0001 to 0.01 volume per cent CH_4. This result points out the difficulty of controlling the composition of the condensed phase by controlling the gas composition above it.

The kinetics of Equations (1) and (2) were studied experimentally in a static system. These data were obtained while attempting to satisfy an immediate need for quantities of uranium carbide powder for sintering studies. Observations were made of the gas pressure within the system as related to time. Pressure data were obtained from manometer readings on a modified Sieverts apparatus containing 30-g batches of uranium metal heated to 700 C by a resistance tube furnace. Initial methane pressures were varied from 90 to 600 mm of mercury.

Attempts to carburize the uranium directly were unsuccessful, possibly due to the formation of a thin oxide film on the uranium by residual oxygen in the system during heating to temperature. The absence of pressure variations during these tests indicated that pyrolysis of the methane at the reaction temperature was, of itself, not significant.

Initiation of the reaction was found to require the hydriding of the uranium and the subsequent decomposition of the hydride during heating to the reaction temperature. It appears probable that decomposition of the hydride produces an activated uranium surface which functions as a catalyst for the decomposition of the methane. The general pattern of the manometric data for the reaction under these conditions is shown in Figure 1. Analysis of the pressure variations as a function of time revealed that the pressure, with the exception of a short initial induction period of from 2 to 4 min, varies linearly as a function of the logarithm of time, as shown in Figure 2.

It appears that the pressure increase is due to hydrogen buildup according to Equation (1), although there are indications that the actual reaction mechanisms involve more than this simple one-step process. The slopes of these plots are independent of the initial methane pressure, increases in initial pressure merely serving to raise the whole plot on the pressure axis. This suggests that the concentration of methane molecules adsorbed on uranium in the range of pressures observed is probably so large as to be almost independent of pressure and that the rate-controlling mechanism involves the solid-state diffusion of either carbon or uranium atoms or both. The local exhaustion of methane in the immediate vicinity of the solid-gas interface would thus be negligible. Indeed, if the term, $\frac{P - P_o}{P_o}$, which denotes the fraction of methane reacted according to the stoichiometry of the above reaction (P being the pressure of the system at any time and P_o being the initial methane pressure), is assumed to be proportional to the fraction of uranium converted into monocarbide, then the rate-controlling mechanism could be inferred as being a diffusion process following a logarithmic rate law similar to that observed in the oxidation of zinc.[9]

However, it was found that when the gaseous products of reaction were evacuated after a time and fresh methane was introduced to the same uranium charge, the original active surface was regenerated and produced coincident pressure-time curves. This

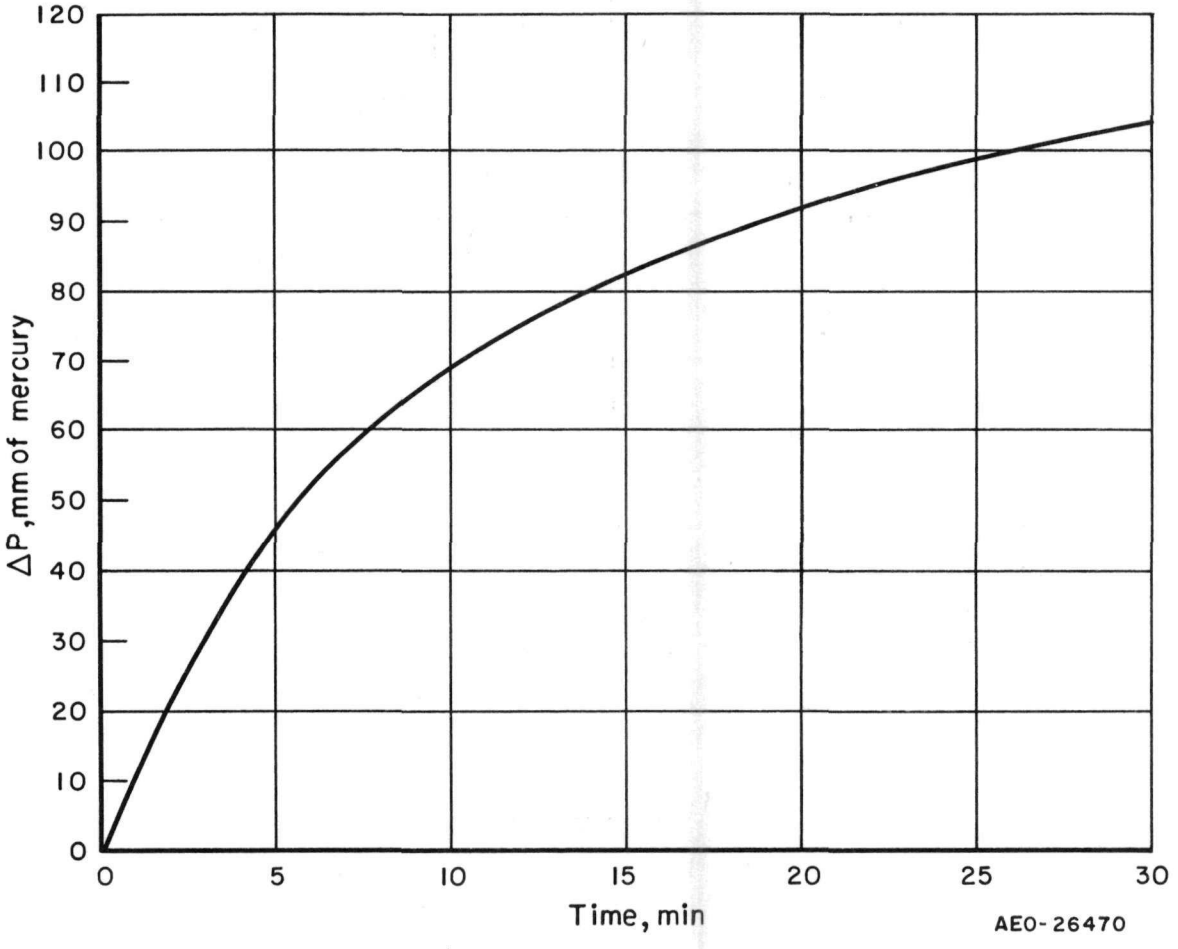

FIGURE 1. GENERAL PATTERN OF THE MANOMETRIC DATA FOR THE URANIUM-METHANE REACTION

The curve illustrated is for data at 700 C with an initial CH_4 pressure of 0.4 atm.

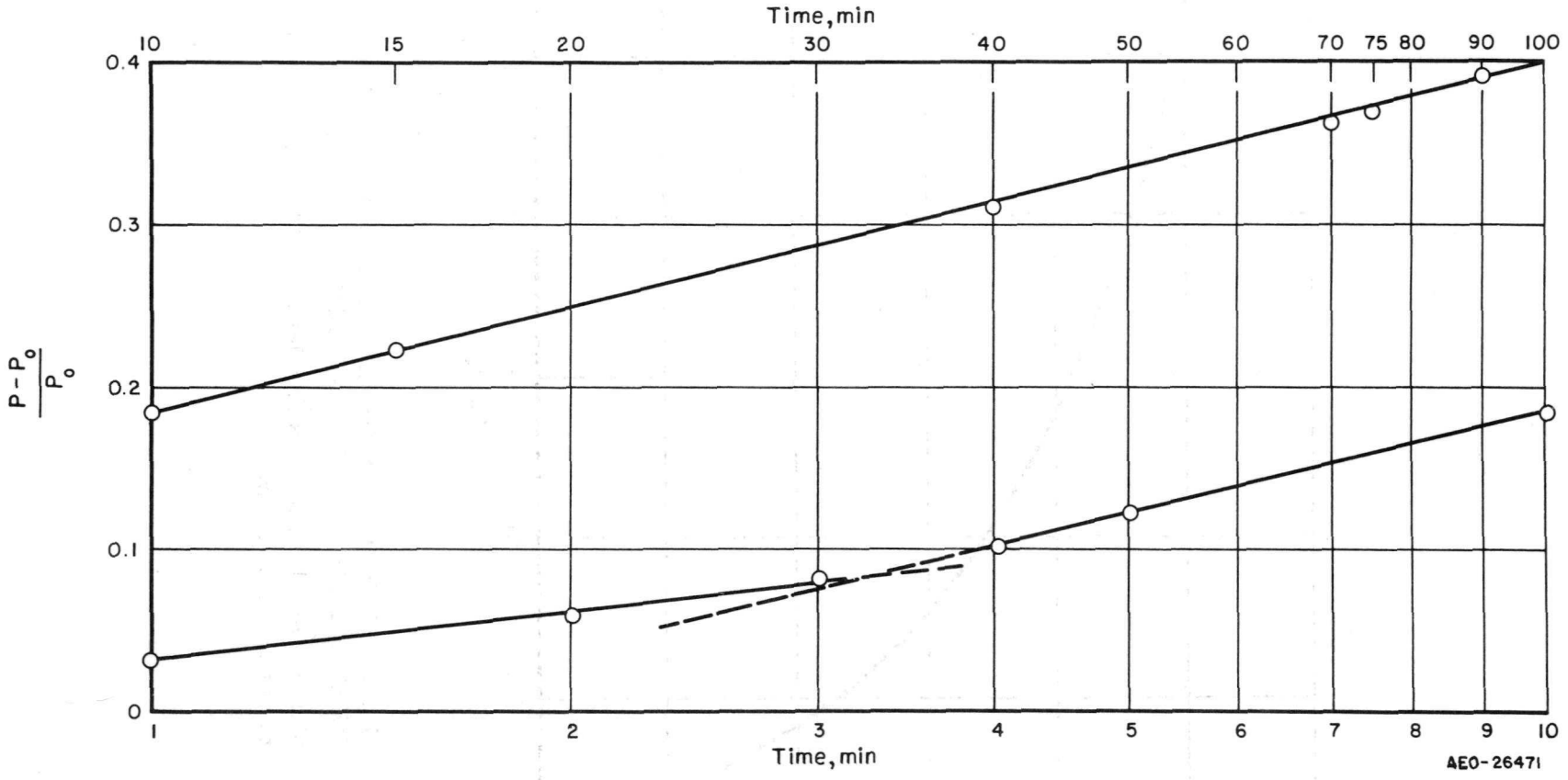

FIGURE 2. FRACTION OF CH_4 REACTED AS A FUNCTION OF TIME (LOG_{10} t)

behavior suggests that the surface reaction is retarded by the preferential adsorption and blocking of reaction sites by hydrogen produced during the reaction, which finally protects the surface so efficiently that further decomposition of methane is practically prevented. An example of such a phenomenon is to be found in the decomposition of ammonia on quartz surfaces.[10]

If this cessation of decomposition is caused by the adsorption of nascent hydrogen on the active surface, an increase in the surface area of the uranium should not only permit the decomposition to proceed further, but should, at the same time, also cause an increase in the initial rate of the decomposition. Differences in the slopes of the pressure-time curves for different uranium charges as well as previously reported variations in the equilibrium constant for the initial pseudo-half-order reaction[11] support this theory. It is considered probably that the uranium carbide behaves as a metal for hydrogen adsorption because of the high density of free electrons observed in UC. The retardation of the methane reaction is probable not caused by any appreciable hydrogenization of uranium carbide by methane because in no case did the calculated hydrogen-methane pressures ratios approach the calculated equilibrium ratio determined from free-energy data for Equation (1).

Thus, in a static system, the available evidence seems to indicate that a surface reaction is the rate-controlling mechanism for the uranium-methane reaction, and that the hydrogen produced by the reaction remains to some extent adsorbed, or associated in some other fashion with uranium carbide.

Preparation by Other Techniques

One batch of this type of powder was prepared with propane substituted for methane. It was felt that no significant differences in the product resulted, although the reaction rate with propane may have been slightly higher.

A mixture which should have resulted in the stoichiometric composition of UC was prepared from UO_2 and carbon powders. This mixture of loose powders was slowly heated to 1500 C in a graphite crucible in a vacuum. The temperature was held at 1500 C until outgassing was completed. X-ray diffraction examination of this product revealed the presence of UC, UO_2, and unknowns. Since a better-quality, finer product was obtained from the alkane reaction, no further work was performed employing this reaction.

Powder was produced at Battelle by arc melting uranium and graphite to form UC buttons and then crushing them in a ball mill or with a mortar and pestle in a protective atmosphere. Three commercial products were studied. These were obtained from the Mallinckrodt, Numec, and Vitro laboratories. The Mallinckrodt material was a minus 20-mesh sinter cake; the Numec material appeared to be arc-melted buttons; and the Vitro material was minus 20 plus 100-mesh spherical shot. These commercial materials were powdered by crushing techniques similar to those used for the arc-melted buttons produced at Battelle.

Characterization of the Powders

Chemical and vacuum-fusion analyses of the various powders are shown in Tables 2 and 3. The Numec material contained 0.31 w/o nitrogen as compared to 0.26 w/o in the Mallinckrodt powder, 0.067 w/o in the Vitro powder, and 0.011 w/o in the Battelle arc-melted and crushed powder. Oxygen contents of these same powders were,

TABLE 2. SUMMARY OF RESULTS OF VACUUM-SINTERING

Chemical and Vacuum-Fusion Analyses, w/o							Average Powder Particle Diameter, μ
Total Carbon		Free Carbon Before Sintering	Oxygen		Nitrogen		
Unsintered Powder	Sintered Compact		Unsintered Powder	Sintered Compact	Unsintered Powder	Sintered Compact	
							Arc-Melted and Crushed
4.94	--	<0.05	0.27	--	0.015	--	20
4.94	--	<0.05	0.27	--	0.015	--	20
4.94	--	<0.05	0.27	--	0.015	--	20
4.94	4.55	<0.05	0.27	0.19	0.015	0.011	20
4.94(b)	4.32	<0.05(b)	0.79	0.36	0.015	0.012	4
4.83	4.66	0.03	0.079	--	0.011	--	25
4.83	4.37	--	0.079	0.14	0.011	--	25
							Commercial
5.33(d)	3.87	0.22(d)	1.33(d)	0.48	0.31(d)	0.32	6
4.89	4.70	0.01	0.19	--	0.31	--	70
6.47	--	0.45	0.40	--	0.26	--	25
6.47	--	0.45	0.40	--	0.26	--	25
--	--	0.10	0.19	--	0.067	--	25
							Methane-Uranium-Reaction
5.98	4.61	0.15	0.69	--	0.15	--	12
5.98	--	0.15	0.69	--	0.15	--	12
5.98	--	0.15	0.69	--	0.15	--	12
5.98	4.32	0.15	0.69	0.15	0.15	--	12
							Propane-Uranium-Reaction
4.68	4.37	0.32	0.56	--	0.16	--	8
4.68	--	0.32	0.56	--	0.16	--	8
4.68	--	0.32	0.56	--	0.16	--	8
4.68	4.17	0.32	0.56	0.17	0.16	--	8
4.85	--	1.1	1.39	--	0.54	--	12(b)

(a) Determined from weights and dimensions.

(b) Estimated.

(c) No great variation in grain size, maximum about equal to average.

(d) Analysis performed after kerosene partly removed by evacuating at room temperature, analysis of same material before adding kerosene in next line.

(e) Ball milled under kerosene.

(f) Static system unless noted otherwise.

(g) Greater than measured value in previous column because fissures from CO release not counted as porosity.

(h) Powder prepared in flowing gas system.

STUDIES ON VARIOUS TYPES OF URANIUM CARBIDE

Sintering Conditions		Compact Density[a], g per cm^3		Metallographic Density, per cent of theoretical	Grain Size,		Comments
Time, hr	Temperature, C	Green	Sintered		Average	Maximum	
Uranium Carbide							
1/2	1700	9.2[b]	10.5	75	30	(c)	--
2	1700	9.2	10.8	80	30	(c)	--
4	1700	9.2	11.5	85	30	(c)	--
2	1900	9.2	11.3	85	35	(c)	--
2	1900	9.1	12.8	90	50	180	--
1	1900	8.8	10.1	75	35	(c)	--
1	1950	8.8[b]	11.2	85	50	125	--
Uranium Carbide							
2	1900	8.8	13.4	95	50	250	Numec[e]
1	1900	9.4	9.6	70	75	(c)	Numec
2	1700	8.0[b]	8.2	70-75	20	(c)	Mallinckrodt
3	1800	8.0[b]	8.2	70-75	20	(c)	Mallinckrodt
--	--	--	--	--	--	--	Vitro
Uranium Carbide[f]							
1	1900	7.3	11.0	75	15	25	--
2	1910	7.7	11.8	95[g]	180	(c)	--
1	1920	7.9	11.9	85	35	180	--
1	1950	7.9[b]	11.2	85	40	125	--
Uranium Carbide[f]							
1	1900	7.2	11.4	80	40	327	--
2	1910	7.4	12.0	95[g]	220	(c)	
1	1920	7.7	10.5	90[g]	50	200	--
1	1950	7.5	--	95[g]	250	350	--
2	1900	7.3	12.5	85	8	375	(h)

TABLE 3. SUMMARY OF RESULTS OF ARGON-ATMOSPHERE SINTERING STUDIES

Condition	Average Powder Particle Diameter, μ	Sintering Conditions: Time, hr	Sintering Conditions: Temperature, C	Density[a], g per cm3: Green	Density[a], g per cm3: Sintered	Metallographic Density, per cent of theoretical	Grain Size, μ: Average	Grain Size, μ: Maximum
1	6	2	1900	8.6	11.1	80	12	(b)
2	25	1/2	1910	8.3	8.4	60	40	(b)
3	25	4	1915	8.8[c]	9.5	70	35	(b)
4	12	2	1900	7.8	10.7	75-80	35	(b)

		Chemical and Vacuum-Fusion Analyses, w/o							
		Total Carbon		Free Carbon	Oxygen		Nitrogen		Uranium
Condition	Type of Powder	Before Sintering	After Sintering	Before Sintering	Before Sintering	After Sintering	Before Sintering	After Sintering	After Sintering
1	Numec, ball milled in kerosene	5.33[d]	4.09	0.22[d]	1.33[d]	0.56	0.31[d]	0.34	95.0
2	BMI, arc melted and crushed	4.83	--	0.03	0.079	--	0.011	--	--
3	BMI, arc melted and crushed	4.83	4.55	0.03	0.079	--	0.011	--	--
4	Methane-uranium reaction	4.88	--	0.31	--	--	--	--	--

(a) Determined from weights and dimensions.
(b) No great variation in grain size; maximum about equal to average.
(c) Estimated.
(d) Analysis performed after kerosene partly removed by evacuating at room temperature; see Table 1 for analysis before adding kerosene.

respectively, 1900, 4000, 1850, and 790 ppm, hydrogen contents were 24, 18, 6, and 15 ppm, and the "free carbon" contents were 0.01, 0.45, 0.10, and 0.03 w/o. The above analyses were obtained on powder of comparable particle size, about 25 μ in average diameter. Further crushing resulted in higher impurity contents. In two typical batches the particle sizes of the product of the static propane-uranium and methane-uranium reactions were 8 and 12 μ in diameter, respectively. Nitrogen contents of these two batches were 0.16 and 0.15 w/o, respectively, oxygen: 5600 and 6900 ppm, hydrogen: 46 and 350 ppm, and free carbon: 0.32 and 0.15 w/o. X-ray examination of the 8-μ powder showed a pattern of UC of very strong intensity, a very faint pattern of UO_2, and very faint patterns of unknowns. The 12-μ powder showed a pattern of UC of very strong intensity, a strong pattern of UC_2, a very faint pattern of UO_2, and very faint patterns of unknowns.

Oxygen was probably the most undesirable impurity present. Where large amounts of oxygen were present, UO_2 was observed in the microstructure. Figure 3 shows the UO_2 distribution in a sintered compact made from powder containing about 1.4 w/o oxygen. During vacuum sintering the UO_2 probably reacts with UC according to the equation:

$$UO_2 + 2UC \rightleftharpoons 3U + 2CO \ .$$

This results in a reduction of the carbon and oxygen contents and in the formation of free uranium and of porosity from the liberation of the CO. In the specimen portrayed in Figure 3, free uranium was present near the surface of the specimen, and the UO_2-UC structure shown in the photomicrograph was present in the center of the compact. Possibly, if the sintering time had been prolonged, the UO_2 in the center of the compact would also have reacted. The microstructure of a sintered compact made from a powder containing 6900 ppm oxygen is shown in Figure 4. As may be seen, no UO_2 is present and the remaining oxygen in the sintered compact (0.15 w/o) is probably dissolved in the UC phase as discussed in the next section. The thickness of this second compact was 1/4 in. The high-oxygen powder compact was 1/2 in. thick.

Nitrogen in the quantities present in the above powders undoubtedly was dissolved in the UC phase in the sintered ompacts, and the amount present before and after sintering remained essentially unchanged. No adverse effects on sintering characteristics due to the presence of nitrogen were observed, although a qualitative difference in resistance to chemical attack by various etches was observed. The high-nitrogen material was less resistant to attack by nitric acid.

No harmful effects caused by the presence of hydrogen were observed during sintering. The largest amount of hydrogen observed in a sintered compact was 42 ppm.

Sintering Studies

The binders used for cold pressing served also to protect the powders from oxidation during pressing and loading into furnaces. The binder was added by immersing the powder in solutions of cetyl alcohol dissolved in petroleum ether, camphor in methyl alcohol, or Carbowax 6000 in methyl alcohol, and evaporating the ether or alcohol under a hood at room temperature after the excess liquid had been decanted.

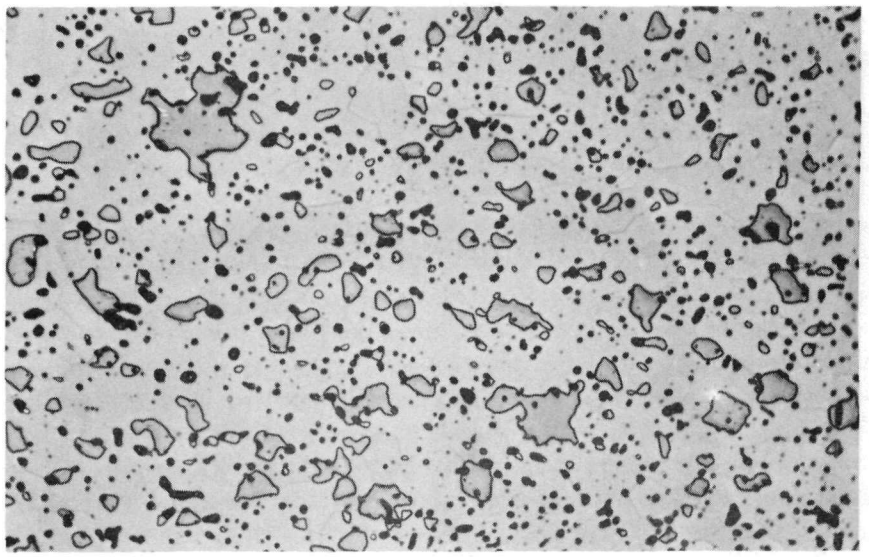

500X N68458

FIGURE 3. MICROSTRUCTURE OF URANIUM CARBIDE CONTAINING LARGE AMOUNTS OF OXYGEN AS AN IMPURITY

This compact, which was made with powder prepared by the methane-uranium reaction and contained 1.39 w/o oxygen, was sintered 2 hr in vacuum at 1900 C. The outlined gray phase is UO_2, the black areas are voids, and the matrix is UC.

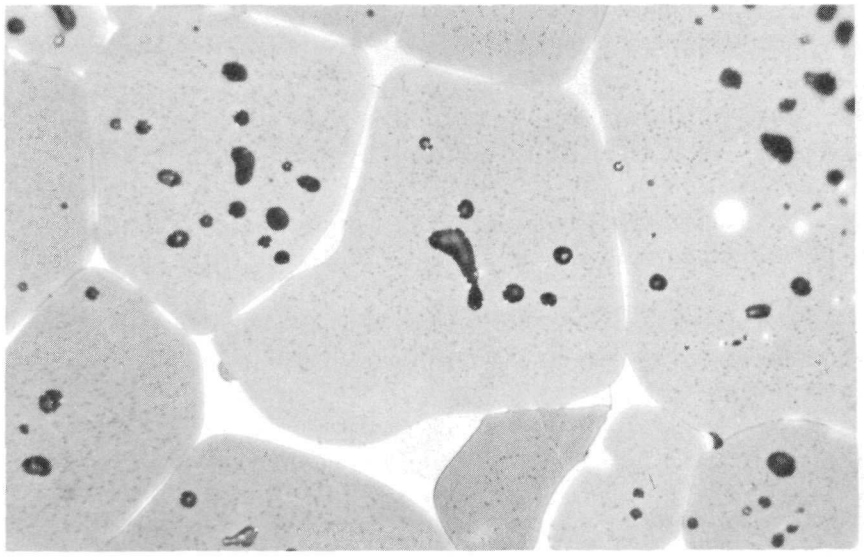

1000X N65945

FIGURE 4. MICROSTRUCTURE OF URANIUM CARBIDE COMPACT PREPARED BY VACUUM SINTERING 1 HR AT 1950 C POWDER MADE BY METHANE-URANIUM REACTION

An oxygen content of 0.69 w/o in the powder prior to sintering was low enough so that it was removed by reaction with the UC to form CO and uranium metal. The oxygen content after sintering was 0.15 w/o. The peppery white particles and the grain-boundary phase are uranium, the black areas are voids, and the matrix is UC. No UO_2 is apparent.

A compacting pressure of 25 to 30 tsi proved to be optimum. The green density of arc-melted and crushed powder having an average particle diameter of 25 μ varied almost linearly between 8.8 and 9.3 g per cm^3 as pressure was varied from 15 to 60 tsi. Sintering was performed in cold-wall vacuum furnaces using tantalum sheet heaters. One of these furnaces was adapted to permit the use of an argon atmosphere. After sintering, density was determined by measuring the dimensions of the specimens and weighing them in air. This technique results in conservative values, since any surface roughness reduces the apparent density as determined by this method. Another density estimate was obtained by microscopic inspection of a polished cross section of the compact. These measurements with estimates of grain size, chemical analyses, and vacuum-fusion analyses are summarized in Tables 2 and 3.

Results of vacuum-sintering studies on compacts prepared from arc melted and crushed powders are summarized in Table 2. Figure 5 is a plot of the time-densification relationship at 1700 C for materials with the 20-μ particle size (Table 2). As may be seen, densification proceeds quite rapidly for the first half hour then tapers off to a much lower rate. Increasing the temperature to 1900 C led to little improvement, as can be seen in Figure 5; a 2-hr interval at this temperature resulted in a measured density of 11.3 g per cm^3 or about 85 per cent dense, as determined microscopically. A photomicrograph of a compact sintered for 4 hr at 1700 C is shown in Figure 6. A homogeneous one-phase structure was typical of about 98 per cent of this specimen. A 50-μ outer rim was observed containing the duplex UC-uranium structure of Figure 4 with slightly larger grains and greater density. An estimated 1 per cent of this rim contained free uranium. As may be seen in Figure 6 spheroidization of pores had barely begun.

The specimens sintered at 1900 C contained spherical voids exclusively, although no appreciable grain growth or pore shrinkage had occurred. The duplex rim of the specimens sintered at 1900 C had enlarged to a thickness of about 250 μ or 10 mils in the 1/2-in.-diameter specimens. Grain growth of many magnitudes and large amounts of grain-boundary uranium were sometimes observed in these rims. It is thought that oxygen from the UO_2 in the specimens and from the small amount of air or moisture in the dynamic vacuum reacts at the surface of the compacts during sintering to reduce the UC to free uranium and CO gas. This sort of reaction has been discussed earlier in connection with impurities and in BMI-1441[12] and could explain the rims observed. Carbon loss by these mechanisms could explain the large drops in carbon content observed, since the oxygen decrease occurring during sintering is not large enough to account for the carbon losses observed.

There was not nearly enough free uranium observed in the microstructure of the compact described in Table 2 as having an average powder particle size of 20 μ and sintered 2 hr at 1900 C to account for the analysis of 4.55 w/o carbon found in the sintered compact. The analytical data in Table 2 indicate that 1900 ppm oxygen and 110 ppm nitrogen were present in this compact after sintering. In other sintered compacts, combined nitrogen and oxygen contents as high as 8000 ppm have been detected, although in each of these cases no microscopic evidence of their presence was detected. As far as nitrogen is concerned, UN is known to be mutually soluble in UC, and therefore, one would expect that relatively large amounts of nitrogen could react with the free uranium in these compacts to form UN which in turn is soluble in UC. No UO phase has been isolated and identified as such, but it would appear equally feasible for small amounts of oxygen to form a substitutional solid solution of the U(C,O) type at concentrations too low for UO_2 to form. The final result is a UC lattice structure with nitrogen or oxygen or both randomly substituted for carbon.

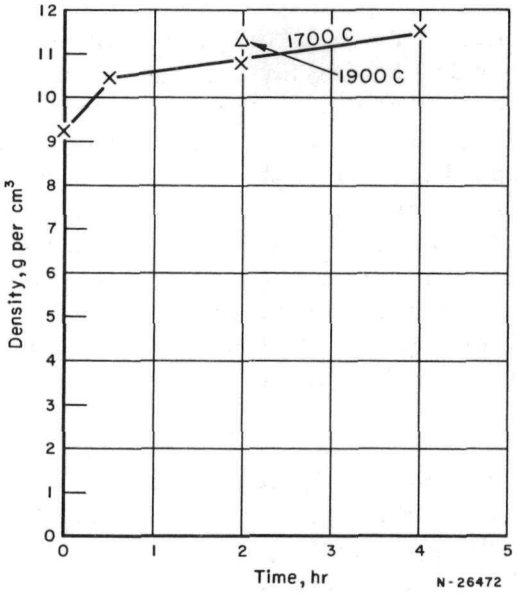

FIGURE 5. EFFECT OF TIME AT TEMPERATURE ON DENSITY OF ARC-MELTED AND CRUSHED URANIUM CARBIDE DURING SINTERING IN VACUUM

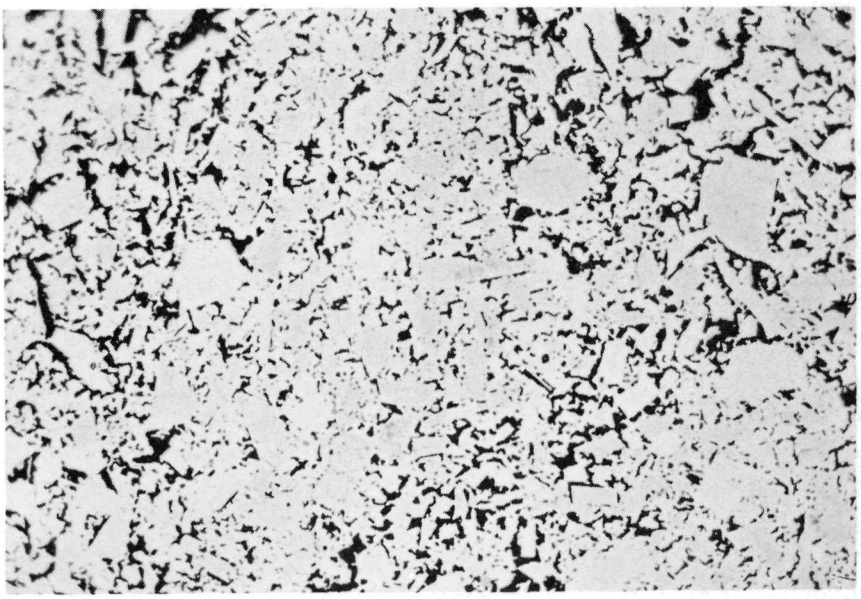

250X N71627

FIGURE 6. MICROSTRUCTURE OF URANIUM CARBIDE COMPACT PREPARED BY VACUUM SINTERING 20-μ POWDER 4 HR AT 1700 C

Black areas are voids. The presence of both rounded and angular voids shows that neck growth advanced in several areas during sintering.

Some of the powder used for the above compacts was crushed further by dry ball milling in argon to an average particle diameter of approximately 4 μ, using uranium balls in a rubber-lined mill. This resulted in appreciable oxygen pickup as may be seen in Table 2. Sintering this material at 1900 C gave compacts having an average density of 12.8 g per cm^3 or 90 per cent of theoretical as determined metallographically. A quantity of grain-boundary uranium was observed in these compacts, as would be expected from the low carbon, nitrogen, and oxygen contents given in Table 2.

An examination of Table 2 shows that higher carbon contents and lower oxygen contents could be achieved by sintering the powders having relatively coarse particle sizes; however, the maximum density attainable for 20-μ-diameter powder was approximately 11.5 g per cm^3. Sintering temperatures up to 2000 C gave no improvement.(14) Crushing to a finer particle size improved the sintered density to 12.8 g per cm^3; however, impurity pickup was greater and the carbon content of the sintered compact was reduced.

The results of tests on commercial powders are also given in Table 2. A maximum sintered density of 9.6 g per cm^3 was observed for the coarse powder. The density of the Numec material after ball milling under kerosene to an average particle diameter of 6 μ was 13.4 g per cm^3 or 95 per cent of theoretical, as determined metallographically, after sintering at 1900 C. The microstructure at the edge and center of these compacts are shown in Figures 7a and b. Free uranium is present as a continuous grain-boundary phase as well as in the form of fine spheroids within the grains. Again, crushing to a fine size has resulted in good densification with the aid of grain-boundary uranium. The microstructure of the 6.47 w/o carbon Mallinckrodt powder compacts after sintering consisted of two phases, UC and UC_2, with no free uranium present.

Sintering studies on the Vitro material have not been completed.

The results of studies on uranium carbide produced by the alkane-uranium reactions are given in Table 2. Since a fine powder was obtained by this method, no further crushing was necessary. The microstructure of a compact of the 12-μ material after sintering at 1910 C is shown in Figure 8. The average diameter of the grains was about 180 μ which represents an order of magnitude growth over the original 12 μ. The only phases present were UC and free uranium, as was the case with all sintered compacts in this series. The measured density of this compact was 11.8 g per cm^3 compared with the metallographic estimate of 95 per cent of theoretical, which is considerably greater than 11.8. The metallographic estimate did not include fissures and voids from CO release which are included in the measured density. Thus, the metallographic estimate gave a truer picture of the fundamental sintering behavior of the material as related to neck growth and pore shrinkage.

Similar structure having higher densities and larger grains were obtained using the 8-μ-diameter powder. Densities of 90 per cent or more were obtained with sintering temperatures of 1910 C or higher, as shown in Table 2. The carbon and oxygen decreases during sintering noted in Table 2 probably resulted from the mechanisms discussed earlier.

A brief study of the effect of using a static argon atmosphere on the sinterability of uranium carbide was conducted. The argon was introduced after heating the compacts in a vacuum to 690 C to remove the binder. Results of these tests are shown in Table 3. The density of the sintered compacts made from 6-μ-particle-size material is seen to be 11.1 g per cm^3. This compares with a density of 13.4 g per cm^3 for the same

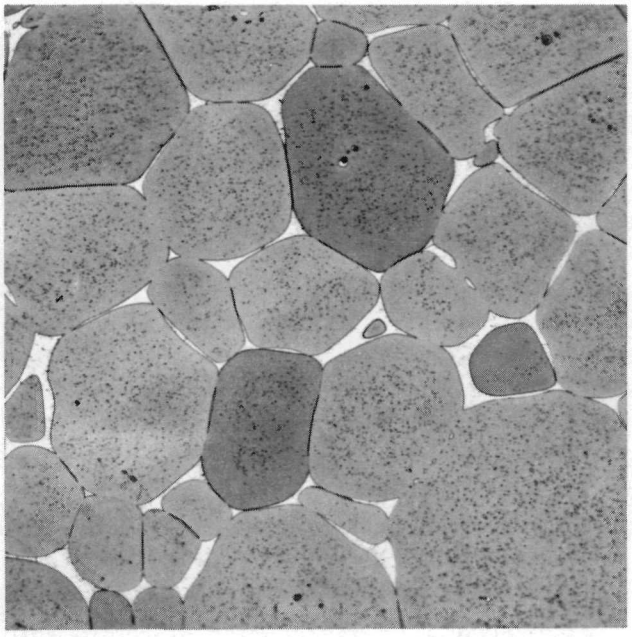

250X N68454

a. Center of Vacuum-Sintered Compact

The white grain-boundary phase and the peppery white phase are uranium.

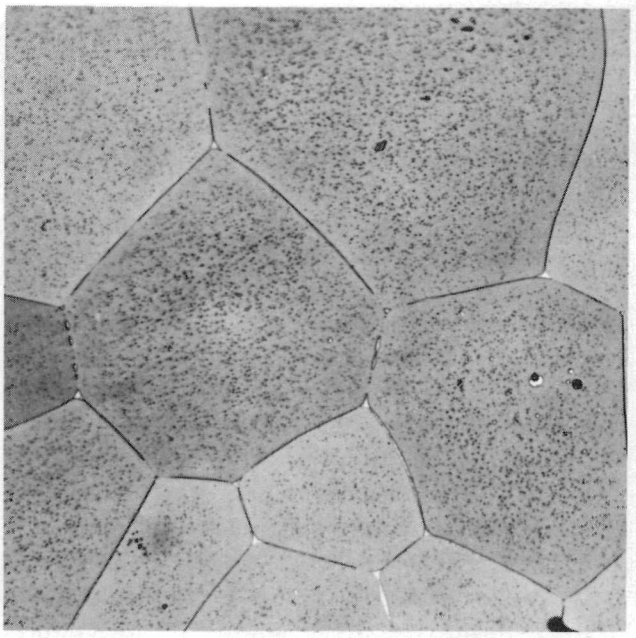

250X N68455

b. Edge of Vacuum-Sintered Compact

This structure shows grain growth and less uranium metal.

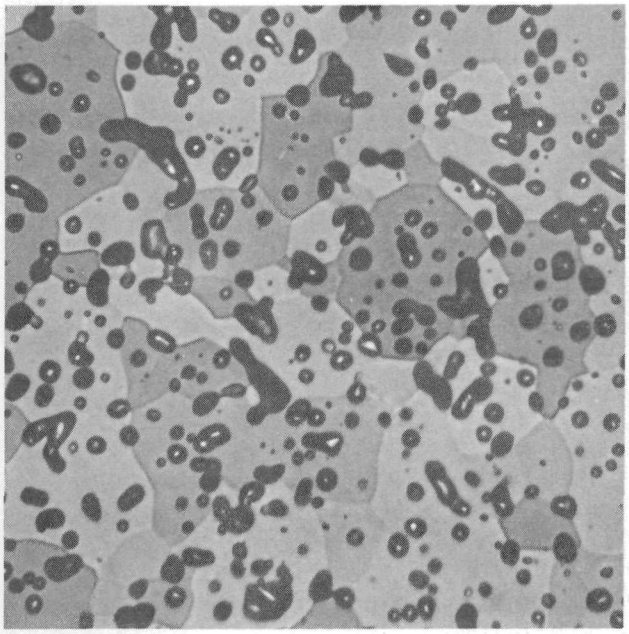

1000X N68460

c. Center of Argon-Sintered Compact

The black areas are voids. The white spots at the center of some voids are light reflections. No uranium is visible.

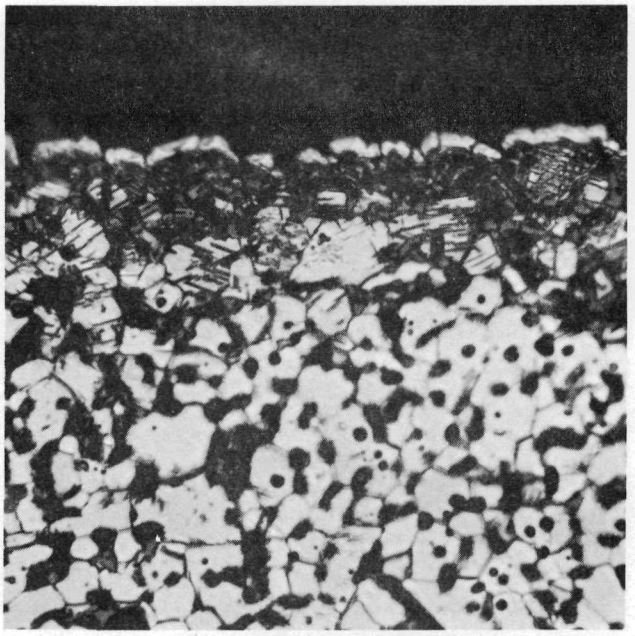

1000X N68461

d. Edge of Argon-Sintered Compact

The unidentified black needles or cracks near the edge resulted from reactions with impurities in the argon such as nitrogen or oxygen.

FIGURE 7. MICROSTRUCTURES OF URANIUM CARBIDE COMPACTS PREPARED BY SINTERING 6-μ POWDER 2 HR AT 1900 C

material sintered in a vacuum, as discussed earlier. Figures 7d and 7c show the microstructure of this material sintered in argon. As may be seen, the use of the argon atmosphere prevented the formation of free uranium and severely retarded grain growth. Minor edge effects to a depth of about 20-μ are shown in Figure 7d. No free uranium was present in this zone. The needlelike structure in the 6-μ rim probably is the result of reactions with impurities in the argon. A comparison of the analytical data pertinent to the above experiments shows that the compact sintered in argon contained more carbon and oxygen. The UO_2-UC reaction discussed earlier undoubtedly proceeds much slower in static argon than in a vacuum. This fact could explain the greater retention of carbon and oxygen when sintering in argon. This difference in carbon and oxygen removal apparently promotes the formation of the hypothetical U(C,O,N) phase discussed previously. The three other experiments described in Table 3 resulted in similar edge and core structures. No free uranium was observed in any of these compacts. A general needlelike precipitate was observed in the sintered compact containing 4.55 w/o carbon, as shown in Figure 9. Although analyses for nitrogen and oxygen were not performed, the microstructure indicates that enough nitrogen or oxygen or both was picked up to form this UC_2-like phase. This UC_2-like phase may also contain various amounts of nitrogen and/or oxygen.

Qualitative examination of the fracture characteristics of a casting of UC-10 w/o Mo_2C alloy showed it to be considerably tougher than pure UC. In addition, this alloy has been found to be much more resistant to corrosion than UC.[13] Sintering theory predicts that ductile materials sinter more readily than brittle materials. Furthermore, the advantages derived from a tougher fuel element are obvious; therefore, arc-melted buttons of this nominal composition were crushed to a particle diameter of approximately 25 μ in an argon atmosphere for sintering studies. Analysis of this powder gave the following results: 4.71 w/o total carbon, 0.21 w/o free carbon, and 9.28 w/o molybdenum. It is estimated that total hydrogen, nitrogen, and oxygen content was about 1000 ppm. Results of vacuum sintering these compacts at temperatures of 1700 to 1900 C are given in Table 4. As may be seen, densities up to 90 per cent of theoretical were obtained with sintering temperatures of 1800 C using this relatively coarse powder. The microstructure of an arc-melted button and that of a typical sintered compact are shown in Figures 10a and 10b. Two phases were observed in the sintered compacts. Microhardness measurements showed the average hardness of the minor phase, shown etched light in Figure 10a and dark in Figure 10b, to be 1380 KHN, compared with 846 KHN for the UC matrix; therefore, on the basis of the possibilities in the three-component system, the minor phase is probably Mo_2C. Pores in these compacts were spherical and were located at Mo_2C-UC interfaces. The structure of the specimens sintered at 1700 C was uniform from edge to center, but depletion of molybdenum and large voids were observed near the edges of the compacts sintered at 1800 and 1900 C. Qualitative tests of an impact nature showed these sintered compacts to be much tougher and less prone to cracking than pure UC. One of the reasons for the better sinterability observed with this alloy was probably connected with the presence of multiple grains per powder particle in this alloy contrasted with the single-grain UC powder.

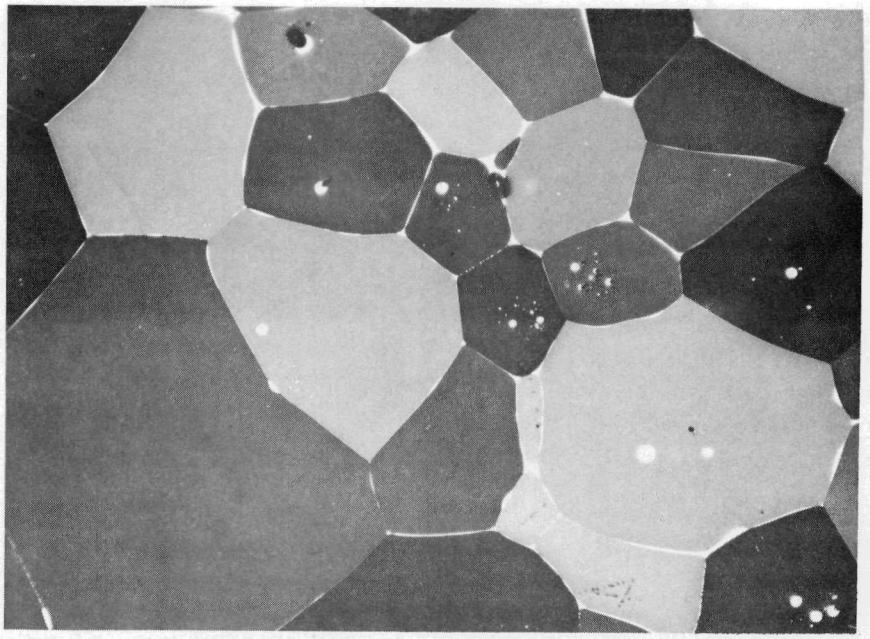

100X N66540

FIGURE 8. MICROSTRUCTURE OF URANIUM CARBIDE COMPACT PREPARED FROM METHANE-URANIUM REACTION POWDER BY VACUUM SINTERING 2 HR AT 1910 C

The phases shown are uranium metal (white) and UC.

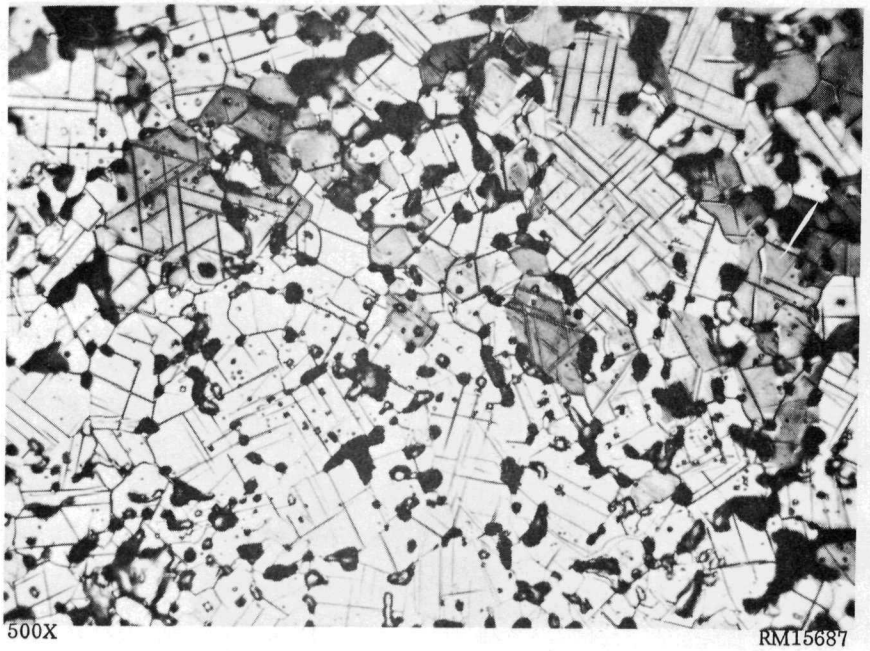

500X RM15687

FIGURE 9. MICROSTRUCTURE OF URANIUM CARBIDE COMPACT PREPARED FROM 25-μ POWDER BY SINTERING 4 HR AT 1915 C IN ARGON

The black rounded areas are voids, the gray and white phase is UC, and the black platelets are probably UC_2. Since this specimen contained only 4.55 w/o carbon, some nitrogen must have substituted for carbon in this structure; thus the structure is really U(C, N) and $U(C, N)_2$.

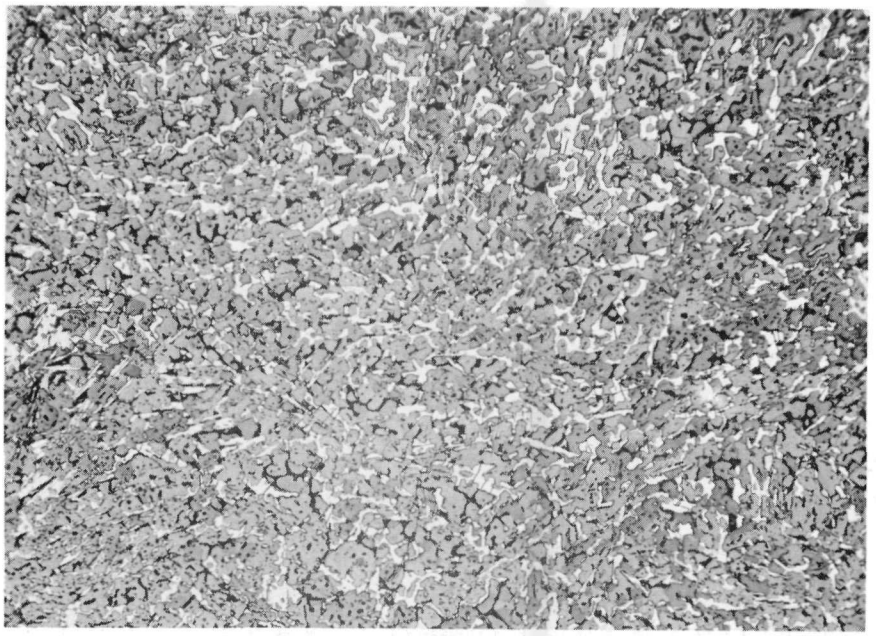

100X Lactic-Nitric Acid Etch N68702

a. As-Cast Button

This structure shows white Mo_2C in a gray UC matrix. The black regions were not identified but are probably voids produced during metallographic preparation.

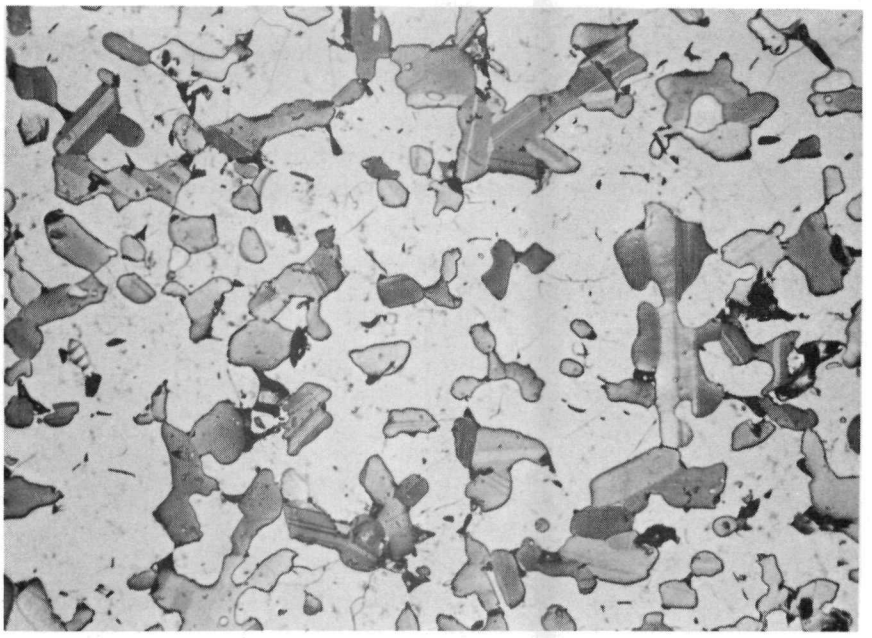

500X Modified Murakami's Etch N70306

b. Compact of Crushed Powder Vacuum Sintered 3 Hr at 1800 C

The structure resulting from sintering powder made from the cast material is shown here. The dark phase is Mo_2C, and the matrix is UC. Note that a different etchant has been used.

FIGURE 10. MICROSTRUCTURE OF UC-10 w/o Mo_2C ALLOY

TABLE 4. SUMMARY OF RESULTS OF VACUUM SINTERING UC-10 w/o Mo_2C AND UC-5 w/o NbC ALLOYS

Nominal Composition	Sintering Conditions: Time, hr	Sintering Conditions: Temperature, C	Density[a], g per cm^3: Green	Density[a], g per cm^3: Sintered	Metallographic Density, per cent of theoretical	Grain Size, μ: Average	Grain Size, μ: Maximum
UC-10 w/o Mo_2C	2	1700	9.1[b]	11.2	80-85	15	(c)
UC-10 w/o Mo_2C	3	1800	9.1[b]	11.9	85-90	15	(c)
UC-10 w/o Mo_2C	2	1900	9.1	11.5	85-90	15	(c)
UC-5 w/o NbC	2	1700	9.1[b]	9.9	--	--	--
UC-5 w/o NbC	3	1800	9.1[b]	9.8	75-80	30	(c)
UC-5 w/o NbC	2	1900	9.1	10.2	75-80	30	(c)

(a) Determined from weights and dimensions.

(b) Estimated.

(c) No great variation in grain size, maximum about equal to average.

Data presented elsewhere in this report show a high ratio of transverse bend strength to compressive strength for a UC-5 w/o NbC alloy. This behavior usually indicates less notch sensitivity, or higher ductility. A button of this nominal composition was arc melted, crushed, and analyzed. The 25-μ diameter powder contained 4.98 w/o total carbon 0.09 w/o free carbon, and 2.80 w/o niobium. Sintering data on compacts of this alloy are given in Table 4. The maximum density achieved was 10.2 g per cm^3 after sintering at 1900 C. No free uranium was observed; and the structures consisted of a single-phase UC-NbC solid solution. These compacts and buttons were not as tough as the UC-10 w/o Mo_2C alloy compacts and buttons.

Early in the program it was learned that the presence of liquid uranium enhanced densification, but, since the melting point of uranium is about 1300 C lower than that of UC, the mechanical properties of a uranium carbide component containing a continuous grain-boundary uranium phase would probably be greatly reduced at high temperatures. It was discovered that liquid-phase grain-boundary conditions could also be obtained by adding chromium to UC and sintering at temperatures above 1760 C. Because of its high vapor pressure, the chromium could be distilled off completely at 1850 C. It was found that the liquid phase sealed voids rapidly at 1760 C. Figure 11 shows the microstructure of a UC-8 w/o chromium alloy after vacuum sintering 1 hr at 1760 C and illustrates the extent of densification. The constituents of the eutectic structure visible in the 1000X photomicrograph are probably UC and chromium. When smaller quantities of chromium were added, local densification was similarly enhanced. The microstructure of an unalloyed UC powder compact vacuum sintered for 2 hr at 1700 C is compared with compacts containing 1 and 3 w/o chromium and also vacuum sintered for 2 hr at 1700 C in Figure 12. Despite the effect on microstructure, the sintering time-versus-density curve at 1700 C for a UC-1 w/o chromium alloy coincided with the curve for pure UC plotted in Figure 5. The reason for this behavior may be found by examining Figures 11, 12a, 12b, and 12c. The spherical, 40 to 80-μ voids in these compacts were caused by the presence of chromium, as these large voids do not occur in pure UC compacts.

A static argon atmosphere was employed in sintering a specially prepared UC-chromium alloy. To minimize the effects of possible impurities in the chromium powder the chromium was added to a uranium-carbon-chromium button by arc melting. The button was then crushed to an average particle diameter of about 25 μ, and green pressed to a density of 9.1 g per cm^3. Chemical analysis of the powder showed 4.97 w/o carbon

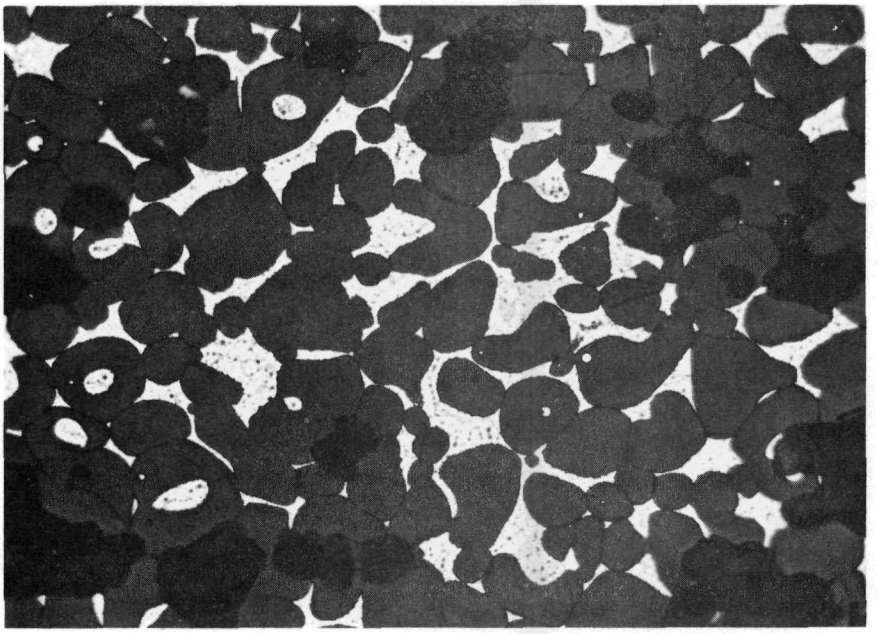

250X N68457

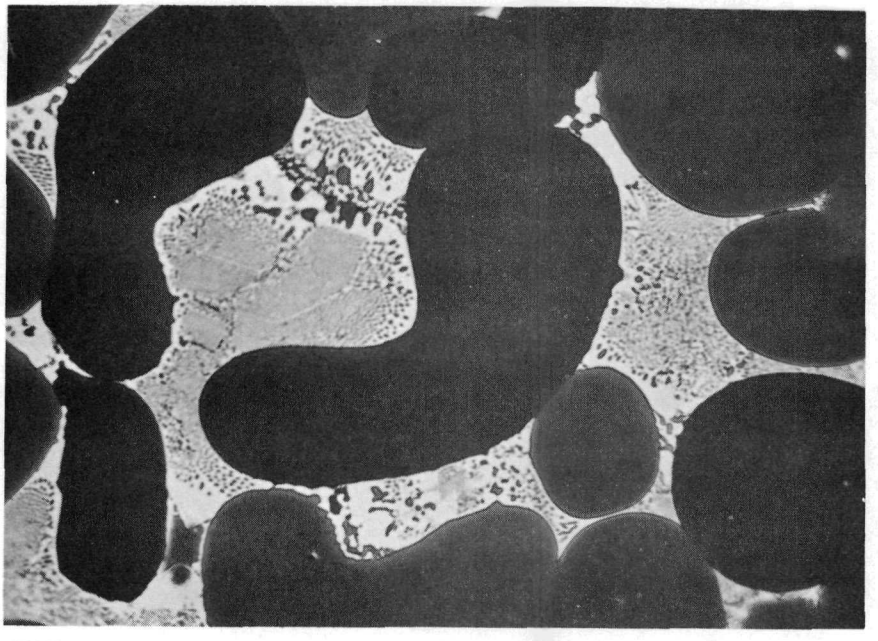

1000X N66544

FIGURE 11. MICROSTRUCTURE OF UC-8 w/o CHROMIUM COMPACT VACUUM SINTERED 1 HR AT 1760 C

The black areas are voids and the gray phase is UC. The white constituent of the eutectic structure around the UC is probably chromium metal, and the dark constituent of the eutectic structure is UC.

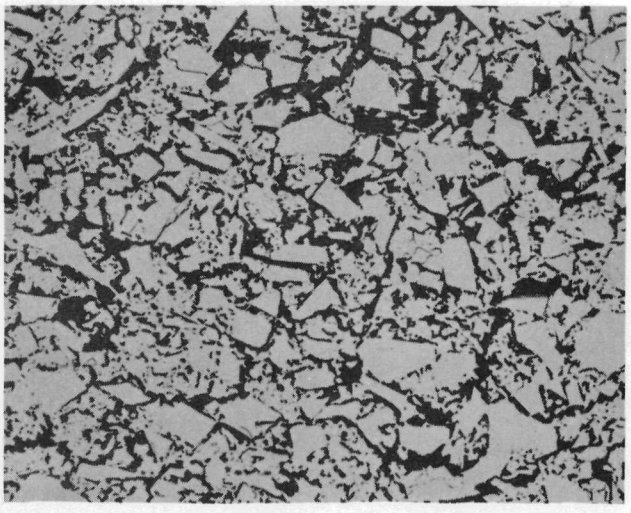

250X N71240

a. Stoichiometric Uranium Carbide

Angular black areas are voids; the remainder is UC.

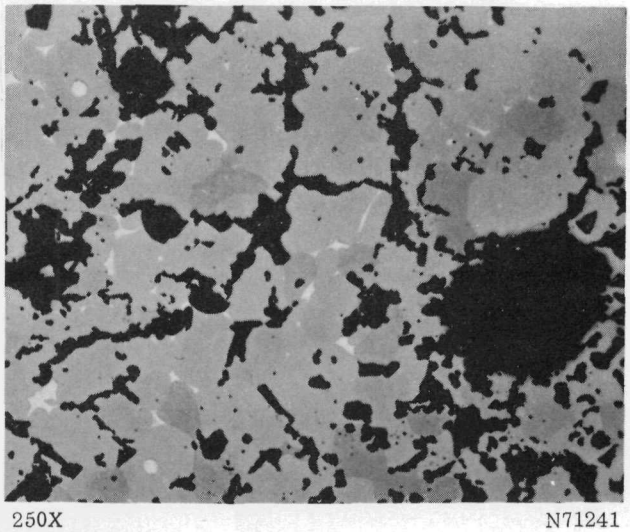

250X N71241

b. UC-1 w/o Chromium

The structure shows advanced neck growth and void rounding. The voids are black, the metallic chromium is white, and the major phase is UC.

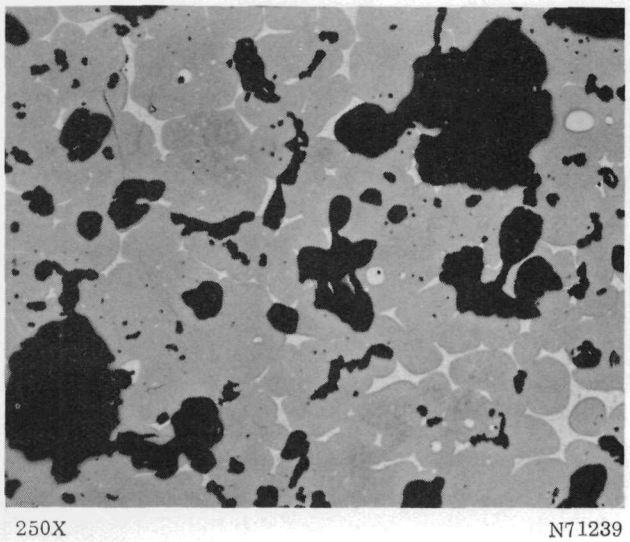

250X N71239

c. UC-3 w/o Chromium

This compact shows more advanced sintering, densification, and rounding of the voids. The metallic chromium in this structure is white, the voids are black, and the major phase is UC.

FIGURE 12. EFFECT OF CHROMIUM ADDITIONS ON THE MICROSTRUCTURE OF URANIUM CARBIDE POWDER COMPACTS SINTERED 2 HR IN VACUUM AT 1700 C

and 1.26 w/o chromium. Compacts of this powder were sintered for 4 hr at 1700 C in an argon atmosphere. Photomicrographs of one of these compacts are shown in Figure 13. The large 60-μ voids visible in Figures 11 and 12 were eliminated. Therefore, it was concluded that these large voids were indeed caused by internal gas pressure. Despite the elimination of the large voids, the average density of these compacts was only 10.5 g per cm^3, similar to that obtained in a vacuum atmosphere. The reason for this may be due to the effect of argon on the sinterability of this ternary alloy or to the nonequilibrium condition of this compact as evidenced by the variable etching effect on the UC shown in the top photomicrograph in Figure 13. Furthermore, this powder was coarser than that used previously.

Hot Pressing

An alternative method to conventional cold-pressing and sintering procedures for densifying uranium carbide compacts consists of applying an isostatic pressure at elevated temperatures while the uranium carbide compact is sealed in an evacuated metal can. Under proper conditions a metallurgical bond may be obtained between the can and the carbide using this method.

A sintered pellet prepared from 25-μ-diameter powder, obtained by crushing an arc-melted button, was densified by this method. The carbon content of this powder was 4.83 w/o. Sintering for 30 min at 1930 C in a vacuum resulted in a density of approximately 70 per cent of theoretical. After isostatically hot pressing this compact in a tantalum container for 3 hr at 1320 C, under a helium gas pressure of 5 tsi, the density of this compact increased to 95 per cent of theoretical, as determined microscopically. Typical photomicrographs of the microstructure near the center of this compact are shown in Figure 14. A small amount of uranium and UC were the only phases present.

Various types of uranium carbides as well as ternary-alloy compacts have been hot pressed in this manner, using niobium tubes and green-pressed and degassed compacts. Microscopic estimates of density are compared with two other methods of density measurement in Table 5. The uranium-carbon-molybdenum alloy powder is the same material discussed previously in connection with sintering of alloys. As may be seen from the table, 3 hr at 1370 C under a 5-tsi pressure densified this material to about 99 per cent of the theoretical density of 12.9 g per cm^3. The microstructure of this compact was similar to that of the sintered structure in Figure 10b except for the presence of an unknown phase, harder than the UC, possibly some modification of U_2C_3. Various diffusion-interaction effects to a depth of 5 mils into the core and 0.2 mil into the niobium tube were observed as a result of the interdiffusion of carbon, molybdenum, niobium, and uranium. No free uranium was present. Although no evidence of oxide was found in this alloy specimen, all of the pure UC specimens referred to in Table 5 contained varying amounts of UO_2. Although no oxygen or carbon analyses were performed on these hot-pressed samples, it is probable that most of the UO_2 observed was present in the starting powder, which contained 2700 and 7900 ppm oxygen in the 20- and 4-μ powder, respectively. The low temperature involved, 1370 C, and the lack of an escape route for CO accounts for the retention of UO_2 as such. In addition to UC and UO_2, 10 to 20 w/o of an unidentified phase, usually associated with the UO_2 was observed. This phase was harder than UC, and was possibly U_2C_3. As may be seen in the table, the densities of four of five pure UC specimens equaled or exceeded 12.5 g per cm^3, regardless of particle size.

250X N71628

Lactic-Nitric Acid Etch

250X N71626

As Polished

FIGURE 13. MICROSTRUCTURE OF COMPACT PREPARED BY SINTERING URANIUM-1.26 w/o CHROMIUM-4.97 w/o CARBON POWDER 4 HR AT 1700 C IN ARGON

The polished structure shows pores as black spots in a white field. The etched structure shows chromium metal to be present as the white phase plus a UC matrix which has retained in part a heterogeneous structure that was observed in the master-alloy casting.

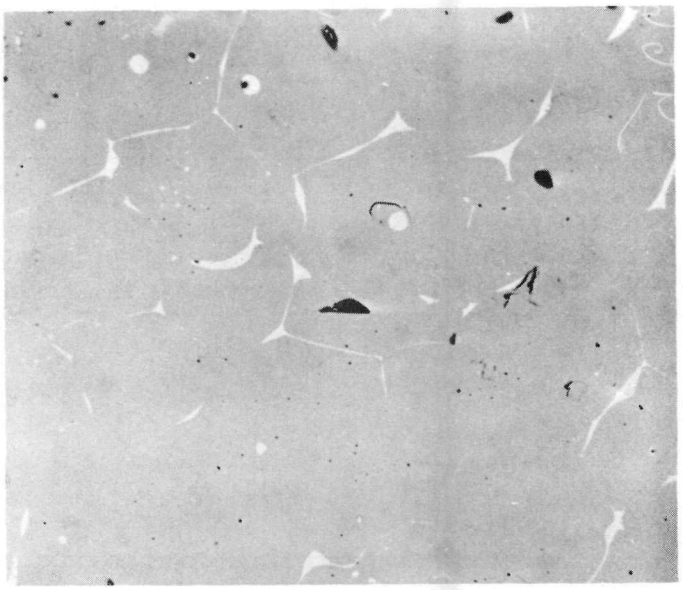

250X RM15918

Bright Field

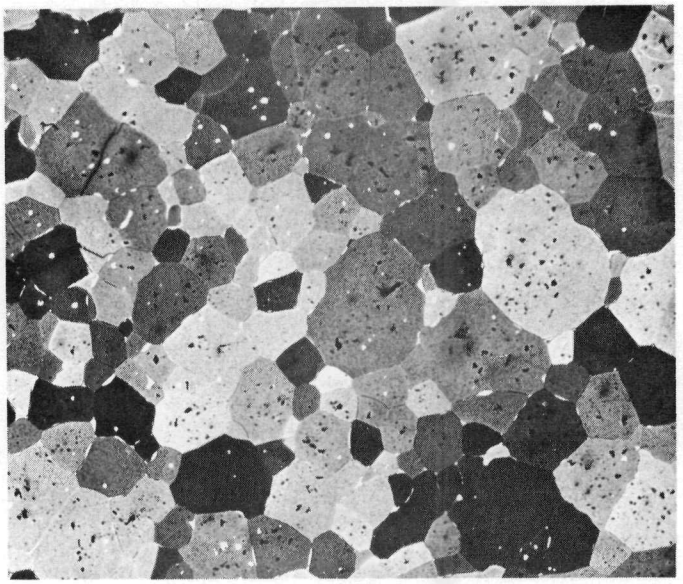

100X RM15915

Polarized Light

FIGURE 14. CENTER OF URANIUM CARBIDE COMPACT ISOSTATICALLY HOT PRESSED 3 HR AT 1320 C AND 5 TSI

These photomicrographs show a structure having a few isolated round pores (black) associated with grain-boundary uranium in a matrix of UC. The average pore volume in this compact was estimated to be 5 volume per cent.

TABLE 5. DENSITY MEASUREMENTS OF URANIUM CARBIDE AND URANIUM-CARBON-MOLYBDENUM POWDER COMPACTS ISOSTATICALLY HOT PRESSED 3 HR AT 1370 C AND 5 TSI

Average Powder Particle Size, μ	Carbon Content, w/o	Molybdenum Content, w/o	Density Measurement		
			Radiographic, g per cm^3	Liquid Buoyancy, g per cm^3	Microscopic, per cent of theoretical
20	4.94	0	12	12.5	90
20	4.94	0	12	12.7	90
20	4.94	0	12	12.9	90-95
4	4.94	0	13	12.8	95-99
4	4.94	0	12	11.6	85-90
25	4.71	9.28	13	12.9	99

Mixtures of minus 100-mesh uranium shot with minus 325-mesh high-purity graphite powder were also isostatically hot pressed in niobium tubes after V-mixing and tamping the loose powder into tubes. A pressure of 5 tsi was applied for 3 hr at 1020 C. Heterogeneous patches of dense uranium-rich areas and powdery graphite-rich areas were the final result. These experiments disclosed, however, that a substantial quantity of UC had formed in the uranium-rich areas, as determined metallographically. Improved mixing techniques will be required for using this method successfully.

Conventional hot pressing of mixtures of 95.2 w/o of minus 325-mesh uranium and 4.8 w/o of minus 325-mesh graphite powder was performed at temperatures ranging from 1050 to 1150 C for 4 hr in a graphite die under a pressure of 2500 psi. Microscopic examination of these specimens showed UC, uranium, UO_2, and two unidentified phases, and the maximum density obtained was 80 per cent of theoretical. No further work was performed using this technique since better results were more readily attainable using the isostatic technique.

Conclusions

Dense uranium carbide components can be fabricated from powders that have an average diameter of less than 8 μ by vacuum sintering compacts of these powders at temperatures greater than 1910 C. Free uranium in the grain boundaries invariably accompanies the high-density (90 to 95 per cent of theoretical) compacts.

Free uranium was eliminated by sintering uranium carbide powders in a static argon atmosphere; however, the maximum density attainable was 85 per cent of theoretical.

Isostatic hot pressing of a partially sintered uranium carbide compact at 1320 C increased the density of the compact from 70 to 95 per cent of theoretical. The structure consisted of UC and free uranium.

Isostatic hot pressing of green compacts prepared from the UC-Mo_2C alloy powder resulted in a density of 99 per cent of theoretical at a temperature of 1370 C and a pressure of 5 tsi compared with 90 to 95 per cent for pure UC.

Alloying UC with Mo_2C improved sinterability. Relatively coarse powder could be densified at 1800 C, and free uranium was eliminated.

Chromium additions to UC greatly enhanced sinterability, but resulted in undesirable side effects. The use of an argon sintering atmosphere gave promise of eliminating the side effects.

MELTING AND CASTING OF UC

Laboratory techniques suitable for the preparation of near-stoichiometric uranium monocarbide shapes of good purity, soundness, and near theoretical density have been developed in past research.[1] However, these laboratory-scale techniques do not appear economically attractive for the production of large quantities of fuel elements. Therefore, within the Fuel-Cycle Development Program attention has been given to the development of techniques capable of volume production of UC. The efforts expended in this particular program of study have been restricted to the examination and development of the inert-electrode skull-type arc-melting technique.

This skull-melting technique utilizes a high-current arc to melt and homogenize the charge materials resting on a bed of the same nominal composition. The molten material is poured from the bed or "skull" into a mold of the desired shape. These operations are conducted within a vacuumtight enclosure to maintain the purity of the product and to protect the charge from oxidation during melting. In this study of skull-type arc melting as it is applied to UC, observations have been made of the effect of furnace atmosphere, melting practice, charge material, and molding practice upon the quality of the product. The composition control obtainable in the product and the homogeneity, purity, soundness, and microstructure of the castings have been evaluated. The results of these activities are presented below.

Furnace, Atmosphere, and Melting Practice

The pertinent novel features of the arc furnace employed in these studies are associated with the crucible that contains the "skull", the mold and the mold-heating device, and the electrode from which the arc is struck and maintained. The crucible is a heavy-walled water-cooled copper container in which the skull is built up by melting small charges of uranium and carbon. The crucible is mounted so that it can be tilted to pour the molten material into an attached mold. When the crucible is in the melting position, the mold can be heated by an induction coil. The graphite electrode tip is internally threaded so that it mounts securely on the copper water-cooled electrode stinger. The shape of the electrode tip is roughly cylindrical, with the working area well rounded.

The power supply is direct current at 24 v (electrode negative), and the current may be varied as desired or as required by the particular procedure used. For example, when the furnace atmosphere used is a dynamic vacuum, the power input to the furnace is initially very low (24 v at 800 amp). This initial lower power input is necessary because of the considerable rise in furnace pressure caused by outgassing of the furnace

and charge. If the pressure is allowed to rise to above 5×10^{-1} mm of mercury absolute, glow discharges occur in the furnace and the melting cycle may be disrupted. As melting is continued and outgassing decreases, the power input is raised to about 2000 amp at 24 v. At this power input, about 300 cm^3 of carbide may be melted and cast. If the arc current is raised to about 3000 amp the volume of molten carbide increases to about 500 cm^3. At any power setting, the volume of material cast is greater using a dynamic vacuum than when a static furnace atmosphere is used.

Charge Materials

Up to the present time, large quantities of prealloyed UC have not been available commercially. For this reason, elemental charges have been used almost exclusively. Usually, reactor-grade uranium and various grades of graphite have been used as charge materials. It has been noted that turbulence and outgassing during melting are related to the purity of the charge materials, particularly the graphite. This effect was also evident on the few occasions when UC scrap from previous runs was remelted. If this scrap was relatively free of oxide, it melted with less turbulence than a charge in which oxide was noticeably present. On the occasions when metallic uranium and spectrographically pure graphite were used as the charge materials, turbulence was very slight.

The nominal composition of the charge is about 4.0 w/o carbon when castings with compositions near 5.0 w/o carbon are desired. The total weight of the charge varies, depending upon the volume of carbide cast from the preceding melt. Approximately 4 kg is charged after a 300-cm^3 melt and 7 kg after a 500-cm^3 melt.

Compositional Control, Homogeneity, and Purity

The problem of control of carbon composition in castings prepared by the skull-type arc-melting technique has received the most attention during recent months. On a laboratory scale, procedures have been developed for preparing uranium-carbon alloys with predicted compositions accurate to ±0.1 w/o carbon. At the present state of development, castings prepared by the skull-type arc-melting technique vary from the intended compositions by ±0.3 w/o carbon. In attaining this degree of predictability with elemental charges of reactor-grade uranium and commercial graphite, melting times, power levels, and skull preparation have been found to be important. In spite of this variation of carbon from melt to melt, the homogeneity of a casting or several castings poured at one time has been very good. Analyses confirm that homogeneities better than ±0.1 w/o carbon are consistently obtained.

With reference to composition control from melt to melt, it has been established that turbulence of the molten pool during melting causes the difficulties experienced. This turbulence is responsible for an uncontrolled pickup of carbon by erosion of the graphite electrode (molten material splatters on the hot electrode and drips into the melt carrying an unpredictable quantity of carbon into the melt). As noted previously, it is evident that impurities in the charge are responsible for the turbulence encountered. At this time no conclusions as to the significance of any specific impurities can be made. However, the lack of turbulence when spectrographically pure graphite is used and the low impurity content of UC melted in a dynamic vacuum would indicate that both metallic

and nonmetallic impurities are responsible. Analyses typical of these materials, graphite, uranium, and UC as prepared in an inert atmosphere and in a dynamic vacuum are presented in Table 6.

Molding Practice and Casting Quality

Interest in molding practice centers around the characteristics that are exhibited by the cast shapes. These include soundness, surface condition, internal structure, and handling characteristics. Both copper and massive (2 in. in OD by 3/4 in. in ID) graphite chill molds have been used. Heated graphite molds also have been used as well as thin-walled (1 in. in OD by 3/4 in. in ID) graphite molds of relatively low heat capacity.

Castings made in copper or in unheated massive graphite molds were prone to cracking upon cooling or to cracking in subsequent handling or machining operations. Cast shapes made in graphite molds heated to a temperature of about 1100 C prior to pouring exhibited the best soundness and handling characteristics. Castings poured in vacuum into unheated thin graphite molds were only slightly inferior in these respects. However, castings poured in a static inert atmosphere into unheated thin-walled graphite molds did not demonstrate as complete a soundness and a freedom from cracking as did castings poured in the same molds in vacuum. This effect is attributed to the more rapid cooling effected by the presence of the inert gas.

The surface condition of the castings was most sensitive to the atmosphere in the furnace. Surface porosity on some ingots was attributed to the static atmosphere present during melting and casting operations under inert gas.

Almost all castings showed evidence of slight primary or secondary center-line shrinkage. In most cases, no deleterious effects of this shrinkage were noted in subsequent handling.

The cast structure of shapes (3/4-in. in diameter by 8 in. long) produced by the thin-walled molding technique usually consists of limited areas of columnar grains at the casting surface. The major part of the castings consist of equiaxed grains. The size of the equiaxed grains is larger at the top of the castings (see Figure 15). A photograph of a typical group of such UC rods cast in a cluster in a thin-walled graphite mold is presented in Figure 16.

The observations noted above apply in general to castings in which the composition is near or above 4.8 w/o carbon (corresponding to UC). Castings containing less than 4.8 w/o carbon show a tendency to hot tear and react with the graphite molds.

Summary of Results and Future Research

The skull-type arc-melting and casting technique appears to be a practical method for producing large quantities of uranium carbide fuel elements. On the basis of the results obtained so far, vacuum melting seems superior to an inert atmosphere because of casting soundness and the larger volume of molten material poured with the same power consumption. Heated molds generally result in castings with better surfaces; however, castings poured into unheated thin-walled molds also have good surfaces. The molten UC

TABLE 6. ANALYSIS OF CARBON MATERIALS, URANIUM, AND UC PRODUCED BY ARC MELTING AND CASTING

	Inert-Atmosphere-Melted UC(a)	Vacuum-Melted UC(b)	Reactor-Grade Uranium	AGSX Carbon	AGOT Carbon	Spectrographic-Grade Carbon
Carbon, w/o	5.0	5.0	0.010	--	--	--
Oxygen, ppm	116	30	30	--	--	--
Nitrogen, ppm	50	50	50	--	--	--
Hydrogen, ppm	6.4	0.6	2	--	--	--
Iron, ppm	50	15	80	--	50	ND
Silicon, ppm	20	25	70	--	60	Trace
Aluminum, ppm	--	20	40	--	<50	ND
Boron, ppm	2	0.5	0.1	10	3	ND
Copper, ppm	20	0.5	10	--	--	ND
Magnesium, ppm	--	2	10	--	10	2
Molybdenum, ppm	5	5	40	--	--	ND
Nickel, ppm	15	2	30	--	--	ND
Calcium, ppm	--	20	20	--	200	Trace
Ash, ppm	--	--	--	6000	400	4

ND = not detected.

(a) Spectrographic-grade carbon used in this casting.

(b) AGSX-grade graphite used in this casting.

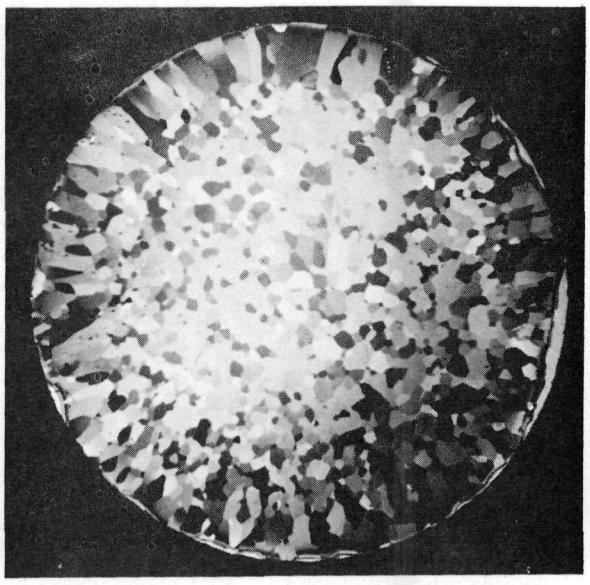

5X N72297

a. Top of Casting

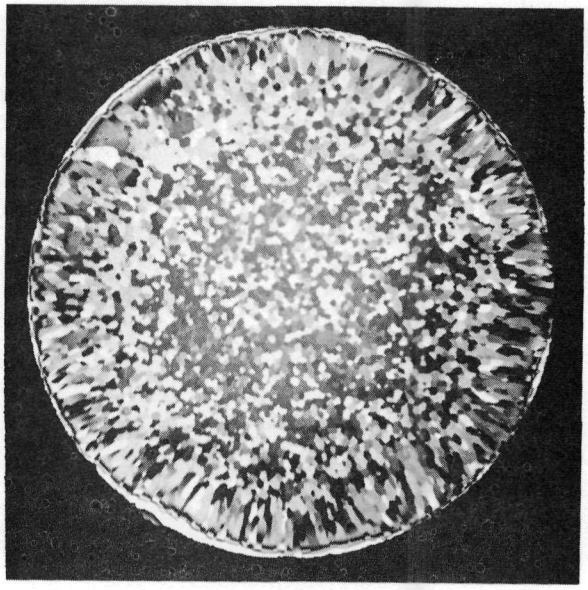

5X N72298

b. Bottom of Casting

FIGURE 15. TYPICAL GRAIN STRUCTURES OF UC CASTINGS PRODUCED IN THIN-WALLED MOLDS

Note columnar grains near surface and difference in grain size between top and bottom.

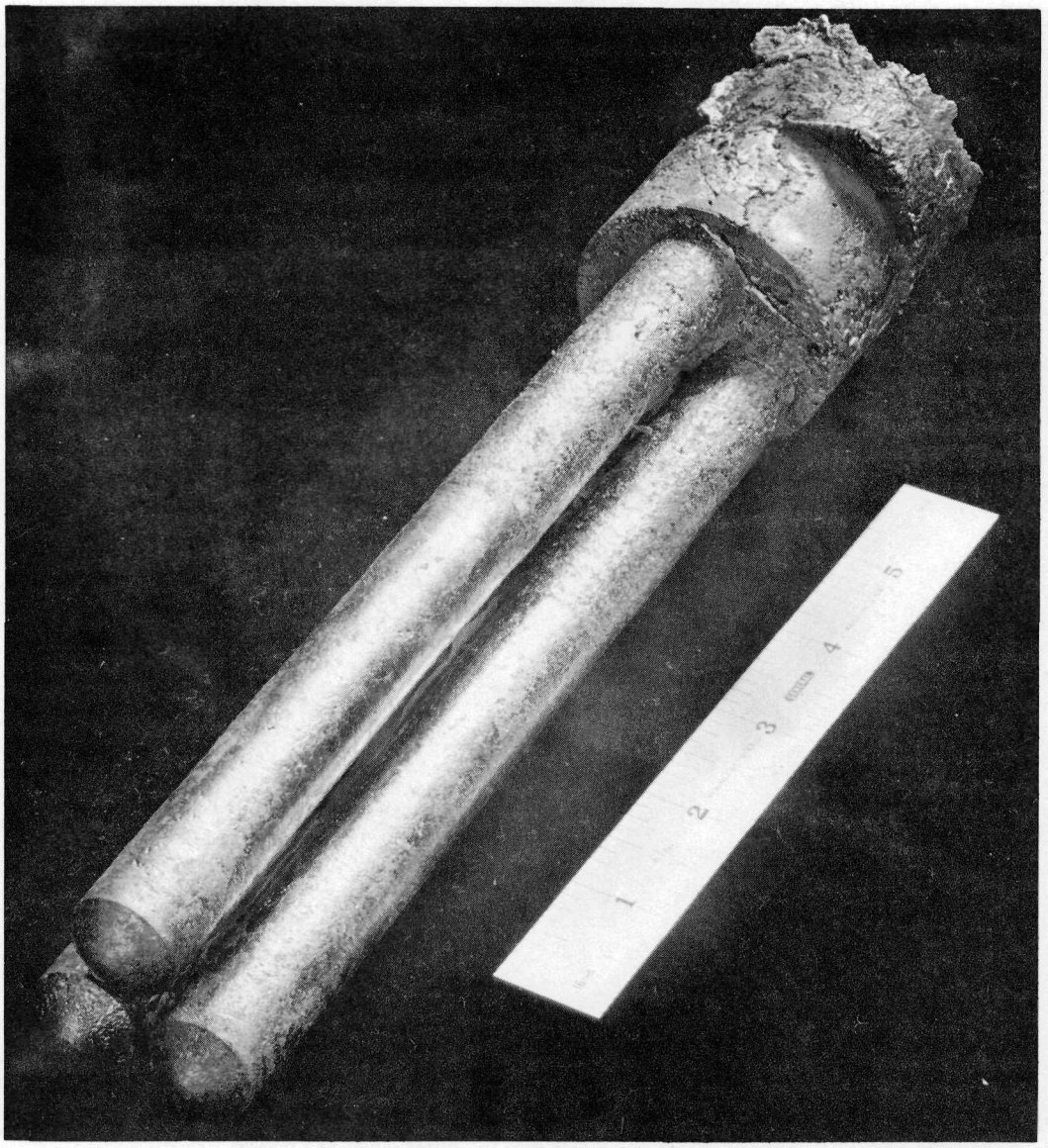

1/3X N67318

FIGURE 16. CLUSTER CASTING OF UC

solidifies very fast in any case, resulting in a structure having columnar grains at the casting surface. Pipe and center-line shrinkage porosity are present in the castings, but this defect is not severe and can probably be reduced for specific shapes.

The problem of most concern is composition control. The main factor contributing to the lack of control is believed to be erosion of the graphite electrode tip by splattering of molten UC. This splattering is caused by turbulence of the liquid during the melting process. The turbulence varies from melt to melt, and results in a variable carbon pickup. Plans for future studies call for the evaluation of various grades of graphite (less costly than the spectrographically pure grade). These various types of graphite will be evaluated both as a charge material and as electrode tips in an attempt to reduce turbulence and improve composition control. Studies of the effect of power levels and furnace atmospheres on composition control are also planned.

MECHANICAL, PHYSICAL, AND CHEMICAL PROPERTIES OF URANIUM MONOCARBIDE

This portion of the program is concerned with the investigation and definition of the character of uranium carbides as potential engineering materials. All physical, mechanical, and chemical properties of uranium carbides which are of engineering significance to reactor construction and which are not specifically covered in other portions of the study are considered to be within the scope of this portion of the program. Some of the areas of interest which have been studied and which are discussed in the following pages include: corrosion resistance in reactor fluids, compatibility with reactor constructional materials, strength, hardness, density, resistivity, and thermal stability, the effects of alloy and impurity conditions upon properties, and the amenability of the carbides to being coated with more corrosion-resistant materials.

During the first 6 months of this research (Phase I), the effects of impurities upon uranium monocarbide were studied. It was found that UO_2 reacted with molten uranium monocarbide to produce a casting containing uranium metal. Presumably, carbon was removed from the melt as carbon monoxide. Small additions of UN to molten uranium monocarbide produced no changes in microstructure, and it was considered probable that the nitrogen remained in the product as the solid solution, U(C,N). Additions of 100 to 800 ppm of iron, silicon, and tungsten to uranium monocarbide produced no changes in electrical resistivity or corrosion resistance. Transverse rupture tests produced data suggesting that these impurities have a more detrimental effect (or less beneficial effect) on carbides nominally containing 5 w/o carbon than carbides nominally containing 4.8 w/o carbon. The average transverse rupture strength of carbides nominally containing 4.8 w/o carbon was 15,000 psi while the average transverse rupture strength of carbides nominally containing 5.0 w/o carbon was 10,000 psi. None of these specimens was analyzed for either carbon or impurity content. A specimen of uranium monocarbide melted under hydrogen showed a corrosion rate of only 250 mg/(cm^2)(hr) in water at 60 C as compared with about 600 mg/(cm^2)(hr) for similar specimens melted under helium. The actual hydrogen and carbon contents of these specimens are unknown and the effect of hydrogen has not been studied further.

The variations of density and resistivity of as-cast samples of uranium-carbon alloys as a function of carbon content were reported in the Phase I report (BMI-1370,

August 1959),[14] and these data are still believed to be essentially correct. These data show a linear decrease in the density of uranium-carbon alloys as a function of atomic per cent carbon up to 9 w/o (66 a/o) carbon (UC_2). The density of UC_2 is about 11.7 g per cm^3. The resistivity of uranium-carbon alloys is essentially constant between 0 and 4.8 w/o carbon at about 35 microhm-cm. Between 4.8 and 9 w/o carbon, the resistivity increases in a parabolic fashion to about 120 microhm-cm at UC_2. This increase in resistivity suggests that UC_2 is slightly less metallic in nature than uranium and UC. The effect of heat treatment upon the microstructure, density, and resistivity of uranium-carbon alloys is described in the following sections.

Binary Uranium-Carbon Alloys

Corrosion tests of uranium-carbon alloys containing 4.5 to 9.25 w/o carbon were conducted in water at 60 C, ethylene glycol at 150 C, and Santowax R (mixed terphenyls) at 350 C. The results of these tests are shown in Table 7. Note that the rates for corrosion in water are per hour while the others are per day. The results shown in Table 7 are for duplicate tests at each composition, one on an as-cast specimen and one on a specimen annealed at 1550 C for 1 hr. The results showed no trend attributable to the heat treament, and for this reason the two tests at each composition have been averaged. The combined results show a distinct trend toward lower corrosion rates near 7 w/o carbon and toward higher corrosion rates near UC (4.8 w/o carbon) and UC_2 (9.2 w/o carbon). This effect is probably related to the higher hardness of alloys containing about 7 w/o carbon.

TABLE 7. CORROSION BEHAVIOR OF URANIUM-CARBON ALLOYS IN WATER AND ORGANIC LIQUIDS

Alloy Carbon Content, w/o	Weight Loss in Corrosion		
	Santowax R at 350 C (1 Week), mg/(cm^2)(day)	Ethylene Glycol at 150 C (1 Week), mg/(cm^2)(day)	Water at 60 C (1 Hr), mg/(cm^2)(hr)
4.5	Disintegrated[a]	66	240
5.0	106	--	Disintegrated[a]
5.9	110	8.9	930
6.8	6	0.6	164
7.2	7	12	108
8.0	7	11	137
8.8	15	50	1330
9.25	15	Disintegrated[a]	460

(a) Specimens initially weighed about 2 g per cm^2 of surface area and tests were 1 week, 1 week, and 1 hr long; so, assuming disintegration just at the end of the test, "disintegration" would correspond to rates of about 300 mg/(cm^2)(day), 300 mg/(cm^2)(day), and 2000 mg/(cm^2)(hr).

When uranium carbides are exposed to moist air for any appreciable length of time, they tend to flake and spall into piles of apparently unoxidized chips. It appears that oxidation proceeds by a stress-corrosion mechanism on certain crystallographic or cleavage planes, and that the chips represent the volumes that have been bypassed by

cleavage facets. This theory would predict that the stress-corrosion process would be retarded by increasing the strength or ductility of the material subject to this process.

It is clear from Table 7 that water attacks uranium carbides of all compositions extremely rapidly even at temperatures as low as 60 C. Unalloyed uranium carbides must be protected from moisture in all forms if the carbides are to be stored for any length of time. Uranium monocarbide normally has a transverse rupture strength of about 10,000 ± 4,000 psi. A sample stored in dry air for 1 month had a strength of 7100 psi. A sample stored for only 1 hr under water at room temperature had a strength of 2400 psi.

The transverse rupture strength (calculated maximum outer-fiber stress in bending) and hardness of as-cast uranium carbides are shown in Figure 17. It is noteworthy that the hardness data show much less scatter and provide a better curve than the data for transverse rupture. This might be expected as a result of the sensitivity of the maximum outer-fiber stress to minor stress raisers in a brittle material such as the carbides. Both curves, however, show a distinct maximum near 7 w/o carbon.

A single value for the compressive strength of uranium carbide castings has been reported.[1] This value plus the results of seven additional tests on UC castings and six new tests on uranium-7 w/o carbon castings are listed in Table 8. These data also indicate an increase in strength from 4.8 to 7.0 w/o carbon.

TABLE 8. MODULI AND COMPRESSIVE RUPTURE STRENGTHS OF URANIUM-CARBON ALLOYS

Alloy Carbon Content, w/o	Compressive Rupture Strength, psi	Elastic Strain at Rupture, per cent	Modulus 10^6, psi
4.8	54,500[a]	0.17[a]	31.5[a]
	45,000	--	--
	80,000	--	--
	46,400	--	--
	40,600	--	--
	35,300	0.13	26.4
	39,600	0.12	32.5
	67,500	0.24	27.6
Average	51,100	--	29.5
7.0	85,400	--	--
	67,600	--	--
	63,400	--	--
	60,400	--	--
	52,600	0.16	32.1
	64,700	0.25	25.9
Average	65,700	--	29.0

(a) Value from Reference (1).

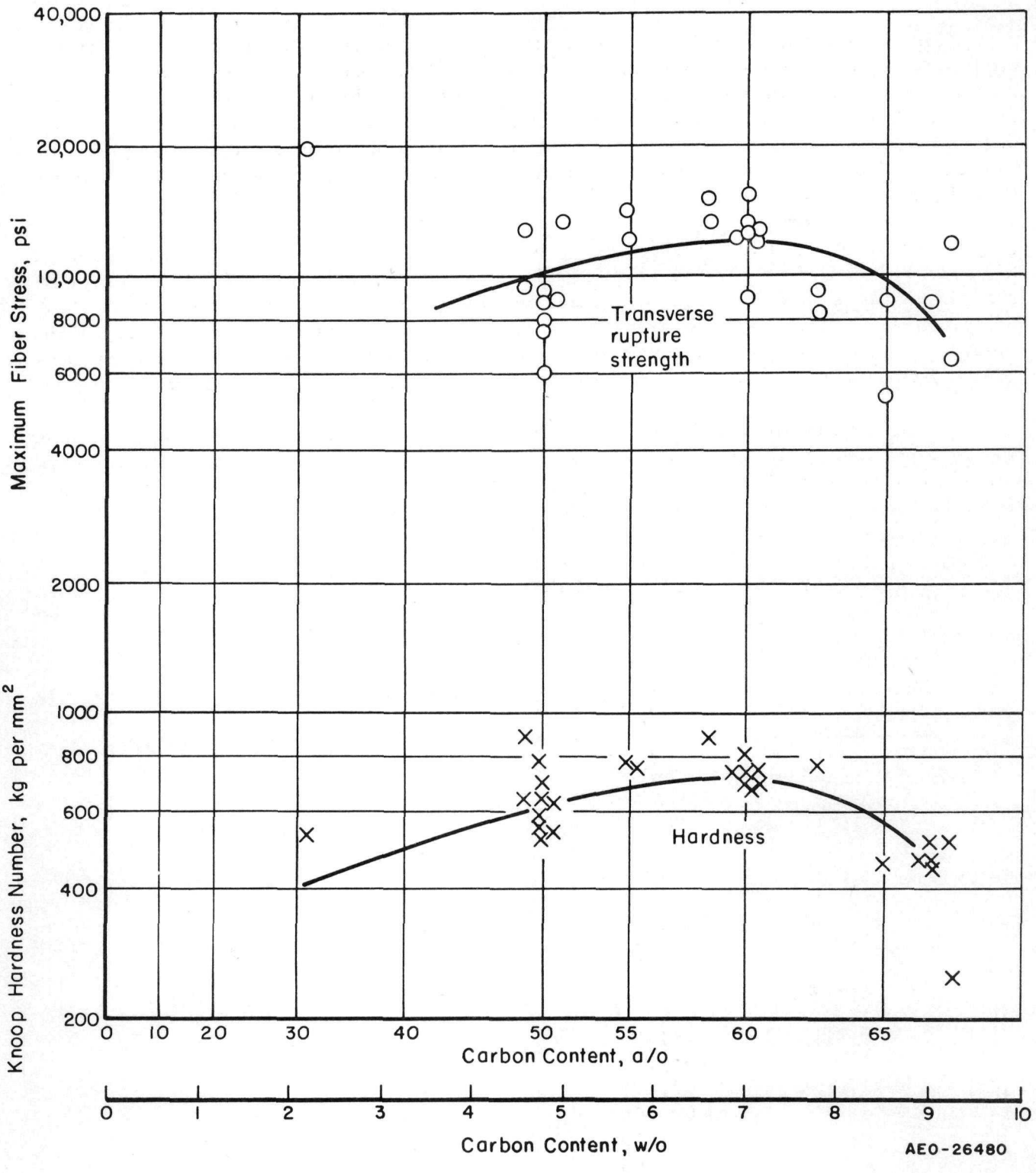

FIGURE 17. TRANSVERSE RUPTURE STRENGTH AND HARDNESS OF AS-CAST URANIUM-CARBON ALLOYS

Many additional data have been obtained with respect to the densities and resistivities of as-cast uranium carbides. No major changes are necessary in the graphs reported in the Phase I report (BMI-1370, August 1959). Several values for the resistivity of uranium monocarbide have been obtained as low as 32 microhm-cm, so a value of about 35 microhm-cm is now considered to be more truly representative of UC than the value of 40 microhm-cm previously reported.

Changes in resistivity, hardness, and density of uranium-carbon alloys have been observed as a result of the formation of the intermediate compound, uranium sesquicarbide (U_2C_3), during heat treatments at various times and temperatures from 1400 to 1800 C. Because these changes are most pronounced in uranium-7.0 w/o carbon alloys and because the results are often ambiguous at other compositions, only the data obtained on uranium-7.0 w/o carbon alloys are shown in Table 9. These data show large increases in resistivity and hardness and a small increase in density accompanying the formation of U_2C_3. The data suggest that U_2C_3 is formed and is stable at all temperatures from 1100 C to approximately 1800 C. Typical values for the resistivity, hardness, and density of U_2C_3 are 210 microhm-cm, 1100 KHN, and 12.8 g per cm .

TABLE 9. PROPERTIES OF URANIUM-7.0 w/o CARBON ALLOYS BEFORE AND AFTER HEAT TREATMENTS TO FORM URANIUM SESQUICARBIDE

Heat Treatment		Resistivity, microhm-cm	Hardness, KHN	Density, g per cm^3
Time, hr	Temperature, C			
As cast (typical)		55	720	12.5
1000	1100	--	1260	--
100	1200	--	1080	--
2	1400	220	1260	12.8
15	1400	200	1080	12.7
1	1500	84(?)	1080	12.7
2	1600	210	1170	12.8
2	1800(?)	210	--	12.6
2	1800(?)	53	741	12.5

The constitutional diagram for uranium-carbon alloys that has been developed in connection with these studies is shown in Figure 18. Typical as-cast structures are shown in Figure 19. Figure 19a is a typical hypoeutectic structure showing primary UC and some intergranular eutectic. Figure 19b is the eutectic structure near 6.2 w/o carbon. Figure 19c is a hypereutectic structure showing primary UC_2 grains decomposed into UC and UC_2 platelets by solid-state reaction at about 1800 C. Figure 19d is typical of the structure of UC_2 in the as-cast condition. The equiaxed grain structure is attributed to the high-temperature allotrope of UC_2; the blocky, twinned structure is attributed to the formation of tetragonal UC_2 at about 1800 C.

Figure 20 shows the structure of an uranium-7.8 w/o carbon alloy after heating for 1 hr at 1550 C. The structure shows a fine-grained dark-etching phase identified as U_2C_3 formed between platelets of residual UC_2. The grain structure of the original high-temperature UC_2 solid solution can still be discerned in this photomicrograph. This

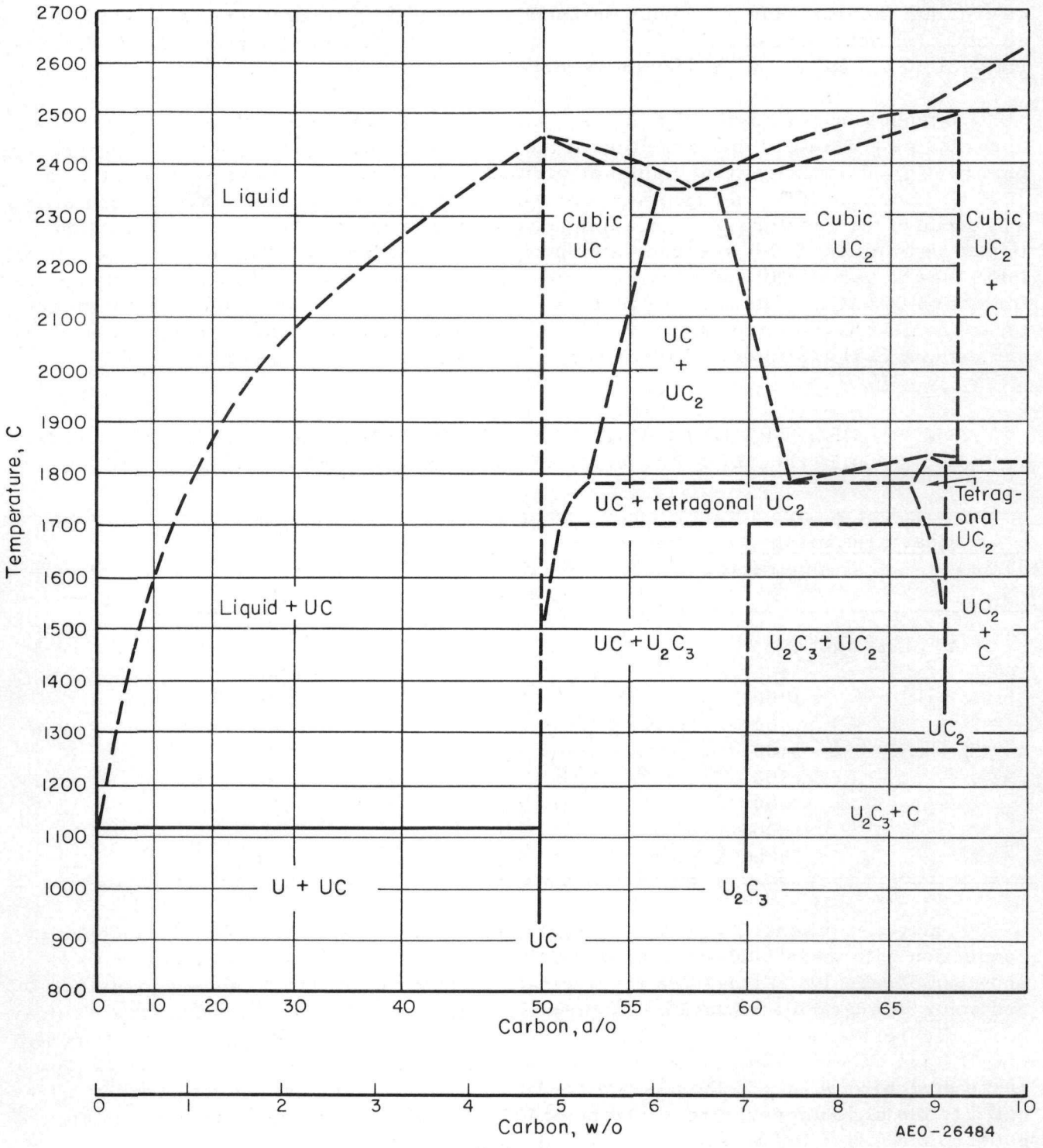

FIGURE 18. URANIUM-CARBON CONSTITUTIONAL DIAGRAM

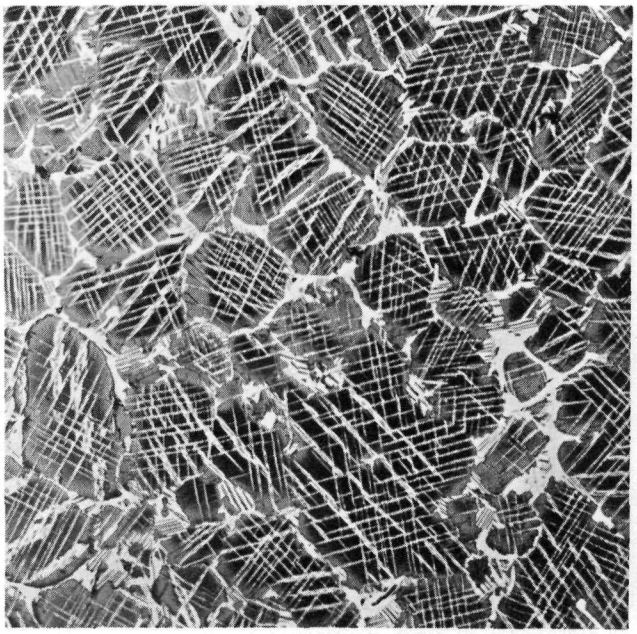

100X RM13086

a. Uranium-5.6 w/o Carbon

This structure is hypoeutectic, showing primary UC and some intergranular eutectic structure.

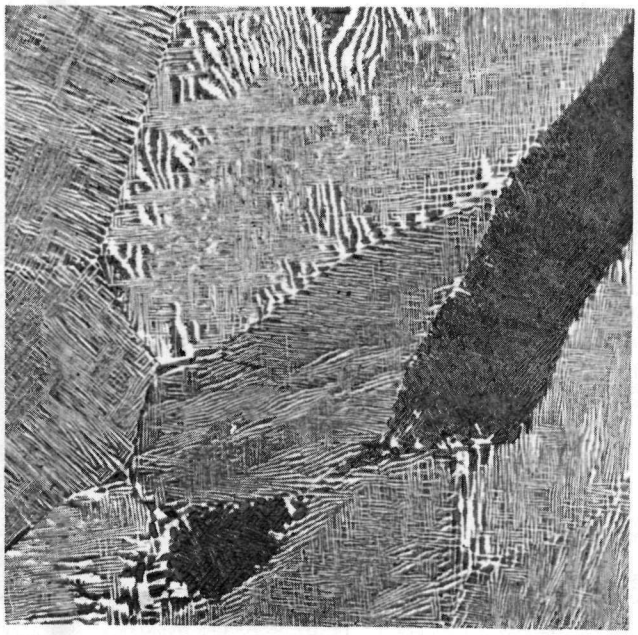

250X RM14551

b. Uranium-6.2 w/o Carbon

This is the eutectic structure.

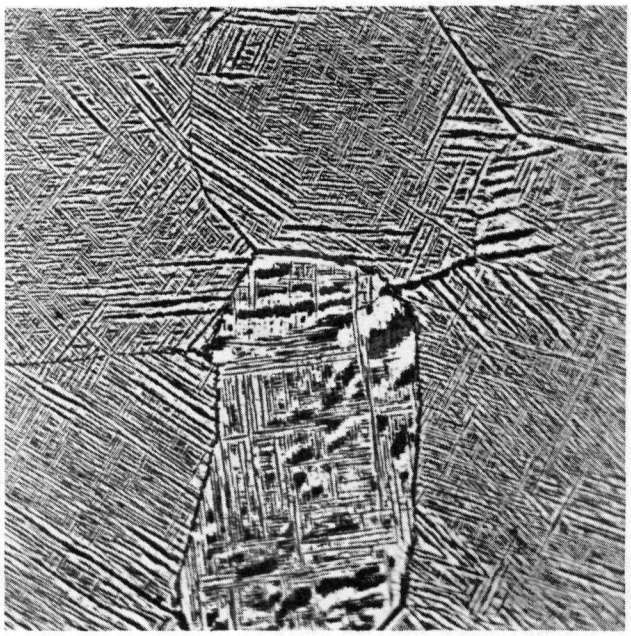

250X RM13814

c. Uranium-6.6 w/o Carbon

This structure is hypereutectic, showing primary UC_2 decomposed into UC and UC_2 platelets.

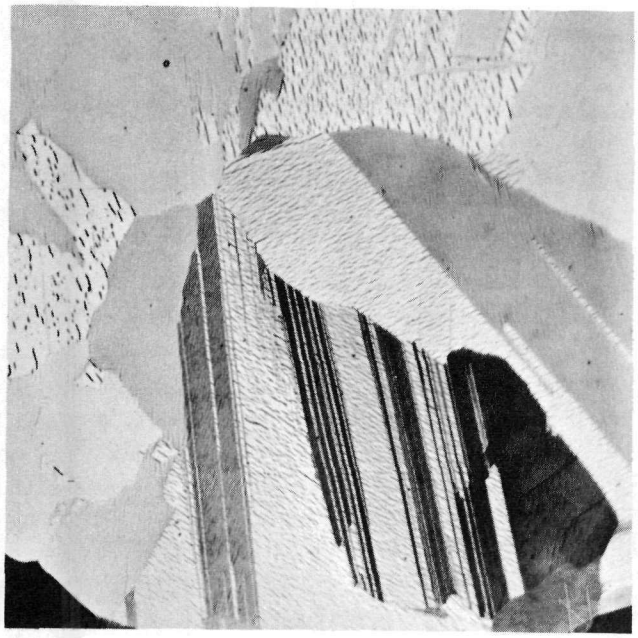

250X RM13821

d. Uranium-8.5 w/o Carbon

This structure is primary cubic UC_2 which has decomposed into parallel plates of tetragonal UC_2 and fine particles of UC.

FIGURE 19. TYPICAL AS-CAST STRUCTURES OF URANIUM-CARBON ALLOYS

structure shows no graphite and establishes that U_2C_3 and UC_2 are in equilibrium at 1550 C. As indicated previously, U_2C_3 is formed readily as a function of time and temperature at all temperatures from 1100 to 1800 C.

Figure 21 shows the structure of a uranium-8.8 w/o carbon alloy after heating for 1000 hr at 1100 C. The black phase is obviously graphite; the mottled, gray phase was identified by X-ray diffraction as U_2C_3, and the twinned, light phase is clearly residual UC_2. Considering the entire cross section of the sample of which Figure 21 is a small portion, it was estimated that only about 20 per cent of the sample had decomposed to U_2C_3 and graphite. This decomposition was also observed to a much more limited extent in samples heated for 100 hr at 1100 and 1200 C. It was not observed in samples heated for up to 15 hr at 1400 C. It is assumed, therefore, on the basis of Figures 20 and 21 that UC_2 is stable above about 1300 C, but decomposes to U_2C_3 and graphite below this temperature. No property changes other than the change in microstructure have as yet been associated with this decomposition.

The compatibility of uranium monocarbide with a variety of metals of reactor construction has been outlined by means of crude tests. The compatibility of uranium monocarbide with liquid NaK alloy has also been studied. The results of these tests are described in Table 10. These results are necessarily qualitative because compatibility depends upon the time involved and the tolerance for contamination in each particular case. The nature of the reaction was investigated for some of these metals. Analyses of the contaminated layers disclosed as much as 1 w/o uranium in the mild steel, 0.4 w/o uranium and 0.5 w/o carbon in the Inconel, 0.9 w/o carbon in the stainless steel, and 10 w/o uranium and 1 w/o carbon in the zirconium. The contaminated layers were harder than the base metal in all cases with the exception of the Inconel. The contaminated Inconel had a larger grain size and significantly lower hardness than the base metal. The nature of the attack on UC by NaK is shown in Figure 22. It is assumed that this effect is caused by residual oxygen in the NaK and is not caused by the NaK itself, since this effect appears to be similar to the attack of moist air on UC noted earlier.

Several attempts have been made to find a satisfactory method of dip coating uranium carbides to protect them from atmospheric attack. Uranium monocarbide rods have been dipped into baths of the following metals and alloys: aluminum-12 w/o silicon alloy, copper, copper-20 w/o silicon alloy, copper-zinc alloy, silver-zinc alloy, and zinc. Wetting of the rods was achieved only with the aluminum-silicon alloy and the copper-silicon alloy. The carbide was dipped in aluminum-12 w/o silicon alloy held molten at 980 C. It was removed after 6 min and examined metallographically. This examination showed that excessive reaction had occurred between the uranium carbide and the aluminum-silicon alloy in this short period. The aluminum-silicon alloy, therefore, appears to have promise as a possible coating for uranium carbides provided that this interaction can be retarded by dip coating at lower temperatures or for shorter times. The carbide was dipped in a copper-20 w/o silicon alloy held molten at 1340 C. It was removed after 2 min and examined metallographically. This examination disclosed a fairly uniform coating of the alloy on the carbide as shown in Figure 23. This photomicrograph discloses that a thin layer of uranium oxide formed on the carbide during the experiment and that this layer was penetrated by the molten alloy. Figure 23 shows the copper-20 w/o silicon alloy at the top and uranium monocarbide at the bottom. Directly in the center is a UO_2 layer which separates the copper-silicon alloy from the carbide. To each side of this UO_2 layer is a white zone of interaction where the copper-silicon alloy has penetrated the oxide and reacted in a superficial manner with the carbide. The UO_2 which was presumably on the surface of the carbide before wetting took place may be seen suspended in the copper-silicon alloy directly above the interaction

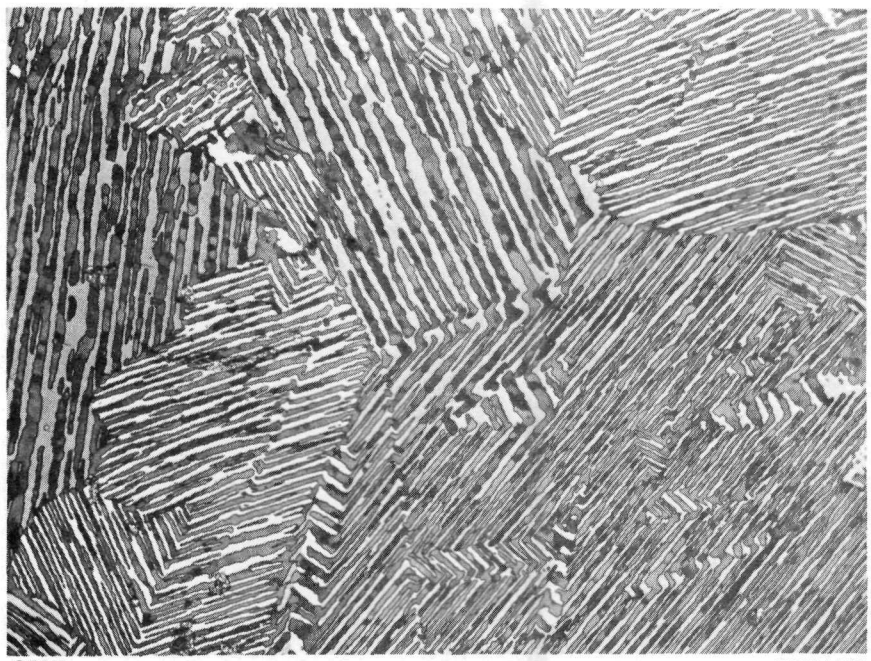

250X RM14463

FIGURE 20. URANIUM-7.8 w/o CARBON ALLOY AFTER HEATING 1 HR AT 1550 C

The structure shows fine-grained dark-etching U_2C_3 between platelets of residual UC_2. The original high-temperature UC_2 solid solution structure is still visible.

250X RM17110

FIGURE 21. URANIUM-8.8 w/o CARBON ALLOY AFTER HEATING 1000 HR AT 1100 C

The black phase is graphite, the gray phase is U_2C_3, and the light, twinned phase is residual UC_2.

TABLE 10. COMPATIBILITY OF URANIUM MONOCARBIDE WITH MATERIALS OF REACTOR CONSTRUCTION

Material in Contact with UC	Test Conditions		Result
	Time, hr	Temperature, C	
Aluminum	24	600	Aluminum contaminated to a depth of 0.005 in.
Copper	24	1000	No reaction
Magnesium	24	600	No reaction
Mild steel	24	1200	Steel contaminated to a depth of 0.020 in.
	24	1000	Steel contaminated (no measurement)
	100	900	No reaction zone observed
	100	800	No reaction zone observed
Molybdenum	24	1200	0.001-in. layer of Mo_2C formed
	24	1000	No reaction
Inconel	24	1200	Inconel contaminated to a depth of 0.030 in.
	24	1000	Inconel contaminated (no measurement)
	100	900	Inconel contaminated to a depth of 0.010 in.
	100	800	Inconel contaminated to a depth of 0.003 in.
Stainless steel	24	1200	Stainless contaminated to a depth of 0.010 in.
	24	1000	Stainless contaminated (no measurement)
	100	800	Stainless contaminated to a depth of 0.005 in.
Zirconium	24	1200	Zirconium contaminated to a depth of 0.030 in.
	24	900	Zirconium contaminated (no measurement)
	100	900	Zirconium contaminated to a depth of 0.005 in.
	100	800	Zirconium contaminated to a depth of 0.002 in.
NaK	720	840	UC oxidized to a depth of 0.010 in.

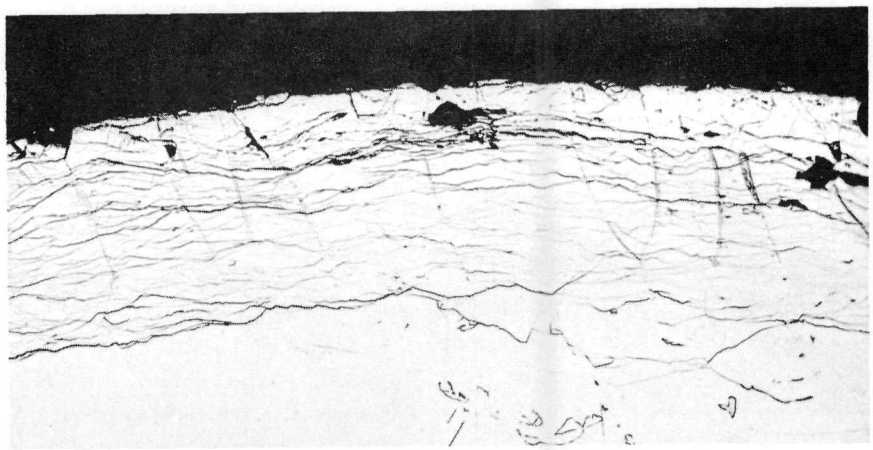

100X RM16647

FIGURE 22. AS-POLISHED CROSS SECTION OF A SAMPLE OF URANIUM MONOCARBIDE EXPOSED TO NaK FOR 1 MONTH AT 840 C

Surface of the UC shows lacework of cracks produced by oxidation.

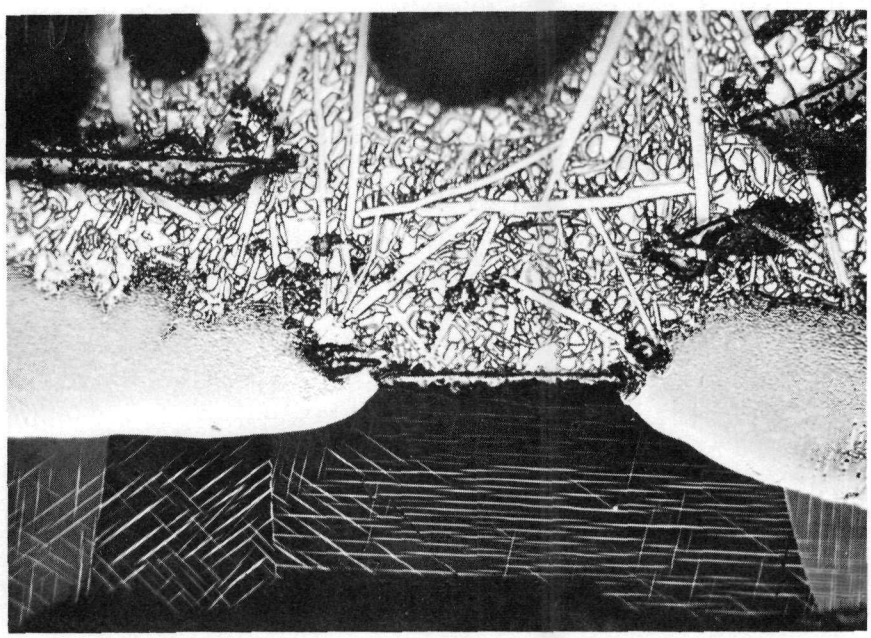

250X RM16451

FIGURE 23. COATING OF COPPER-20 w/o SILICON ALLOY ON URANIUM MONOCARBIDE PRODUCED BY DIPPING FOR 2 MIN AT 1340 C

Top third of photograph shows the copper-silicon alloy, bottom third shows UC. Between is a thin film of UO_2 and thick white zones of interaction.

zones. Future dip-coating experiments will, therefore, be based on the assumption that any coating alloy must contain an element such as aluminum or silicon which will react with uranium oxide.

Ternary Alloys of Uranium and Carbon

Primarily as an attempt to improve the storage, handling, and corrosion resistance of uranium carbides various alloying elements have been added to them. The alloying elements have all been added as metals to melts containing various amounts of carbon. It was assumed that where sufficient carbon was present to form carbides, the carbides would form from the metal upon solidification. Excess metal was intentionally added in many instances. An attempt was made to make alloys based on uranium plus 4.8, 7.0, and 9.0 w/o carbon plus 0.5, 1, 5, 10, and 20 w/o of aluminum, chromium, iron, manganese, molybdenum, nickel, niobium, tantalum, titanium, tungsten, vanadium, and zirconium and their carbides. Alloys containing appreciable amounts of aluminum and manganese could not be made because of the high vapor pressures of these elements at the melting points of the uranium carbides. The alloys containing chromium, iron, nickel, and zirconium and their carbides usually did not produce castings of sufficient soundness to prepare specimens for property studies.

Property data obtained on some of the more promising alloys of uranium monocarbide are shown in Figures 24, 25, and 26. Alloying produced a similar improvement in the properties of uranium-7 w/o carbon alloys and uranium-9 w/o carbon alloys. Typical properties of uranium monocarbide-base alloys containing niobium and niobium carbide are shown in Table 11. These data show a clear trend of increasing strength and hardness for the alloys with increasing alloy content. A trend toward increasing corrosion resistance with increasing alloy content is masked somewhat by the scatter of the data. The trend becomes clear, however, if the data in Table 7 are compared with the data in Figure 24 and in Table 11. The corrosion rate of unalloyed UC in Santowax R at 350 C apparently may vary from about 0.4 mg/(cm^2)(day) to over 100 mg/(cm^2)(day), depending upon unknown conditions. The corrosion rate of UC containing 10 w/o of a refractory metal or metal carbide apparently may vary from about 0.1 mg/(cm^2)(day) to perhaps 1 mg/(cm^2)(day), according to the data shown in Figure 24. As has been mentioned earlier, it is probably more than coincidental that the increased corrosion resistance of the alloyed carbides is associated with increased strength and hardness.

Examination of these alloys by metallographic techniques did not disclose any structural reason for the improvement in corrosion resistance with alloy content. Photomicrographs of the structures of the more promising alloys are shown in Figure 27. The massive dark phase in Figure 27a is primary uranium monocarbide; the remainder is a eutectic consisting of dimolybdenum carbide and uranium monocarbide. The solid-solution structure of uranium monocarbide and niobium monocarbide shown in Figure 27b is so severely cored that it appears to be two distinct phases; the white areas are presumed to be rich in niobium. The alloy shown in Figure 27c is apparently close to a eutectic between uranium monocarbide and titanium carbide; the white particles are presumed to be primary titanium carbide. The structure shown in Figure 27d is analogous to that shown in Figure 27a; the massive, dark phase is primary uranium monocarbide; the white areas are believed to be an unresolved eutectic between uranium monocarbide and vanadium carbide.

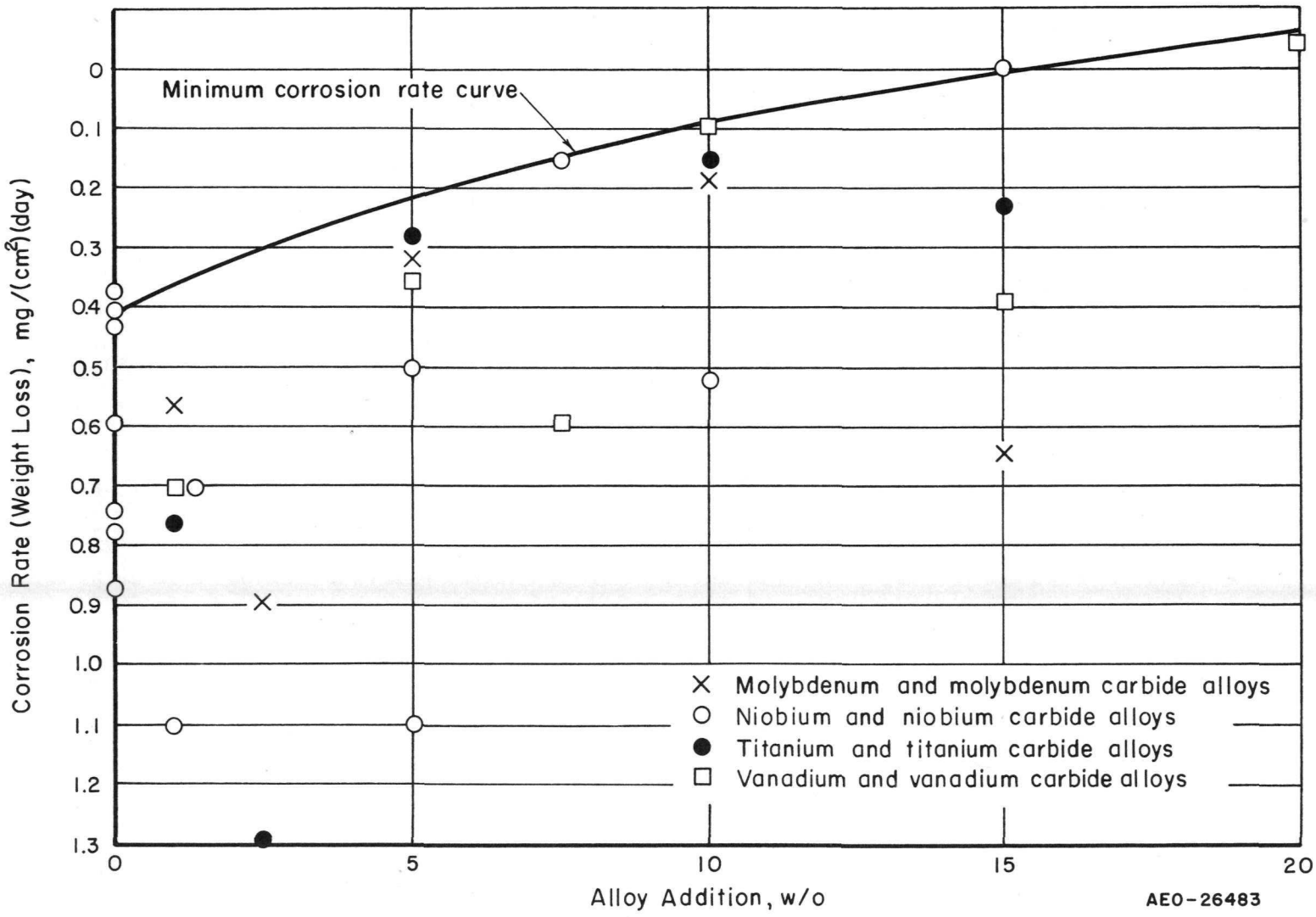

FIGURE 24. CORROSION OF ALLOYS OF URANIUM MONOCARBIDE IN SANTOWAX R AT 350 C

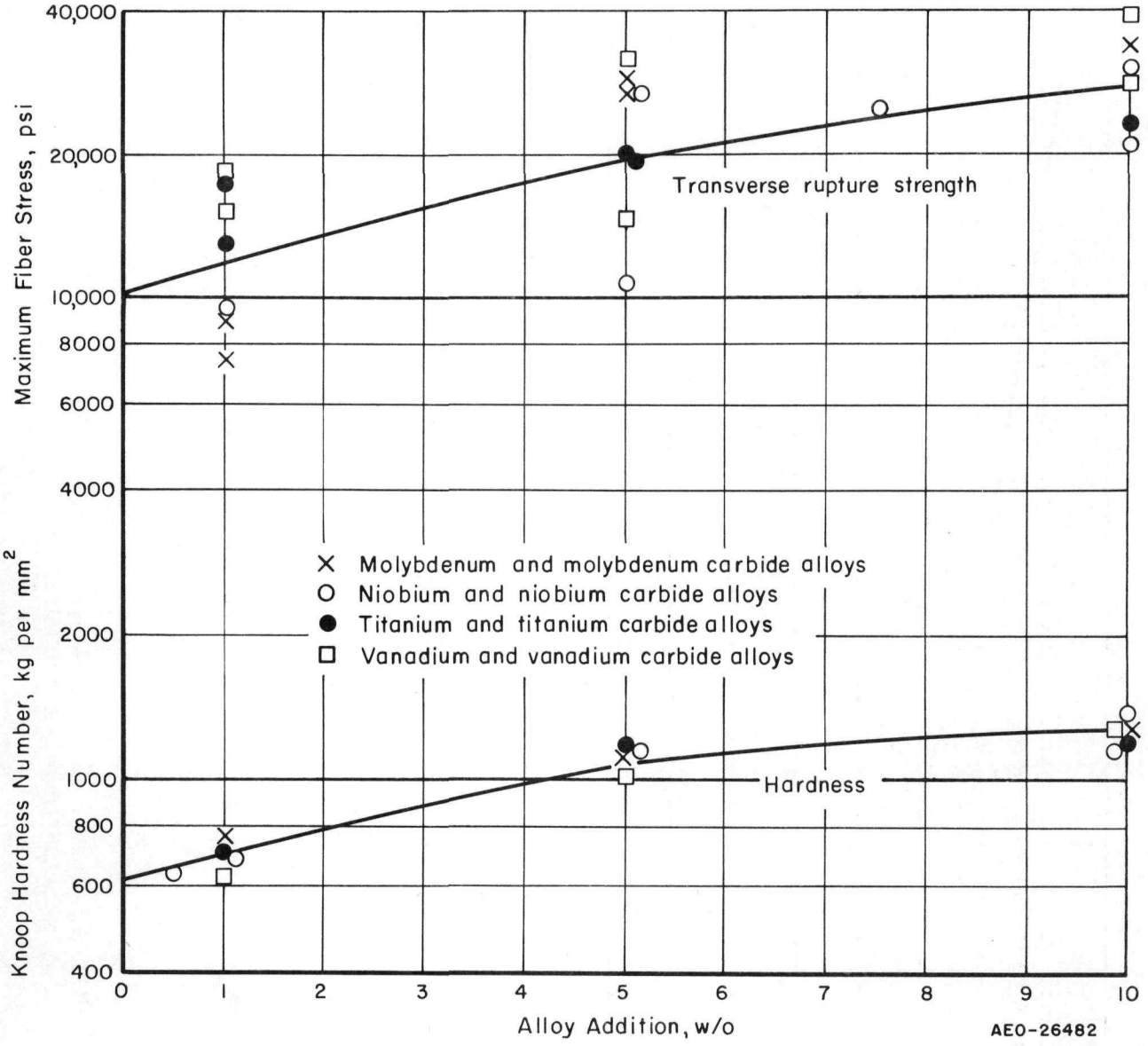

FIGURE 25. TRANSVERSE RUPTURE STRENGTH AND HARDNESS OF AS-CAST ALLOYS OF URANIUM MONOCARBIDE

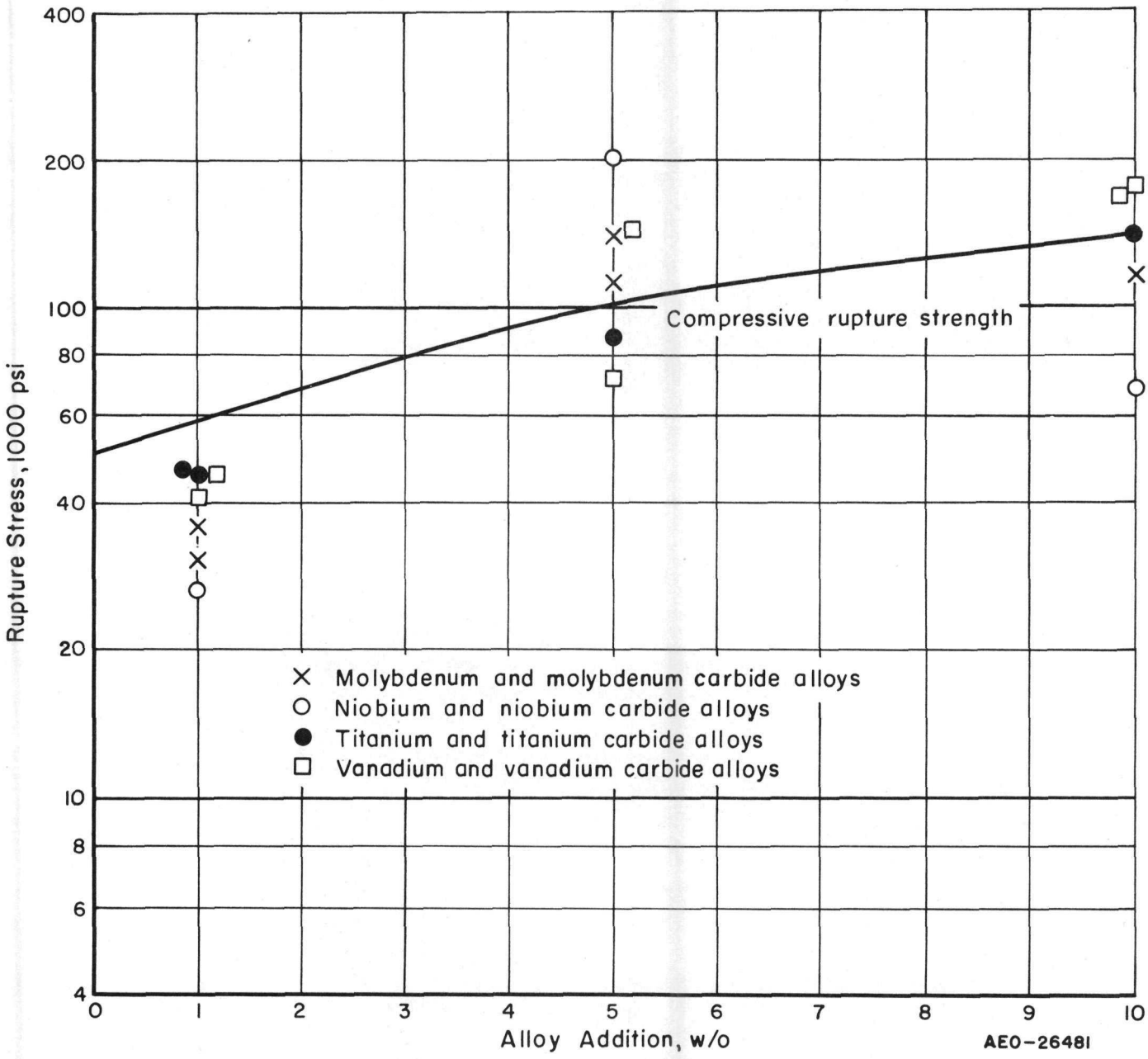

FIGURE 26. COMPRESSIVE RUPTURE STRENGTH OF AS-CAST ALLOYS OF URANIUM MONOCARBIDE

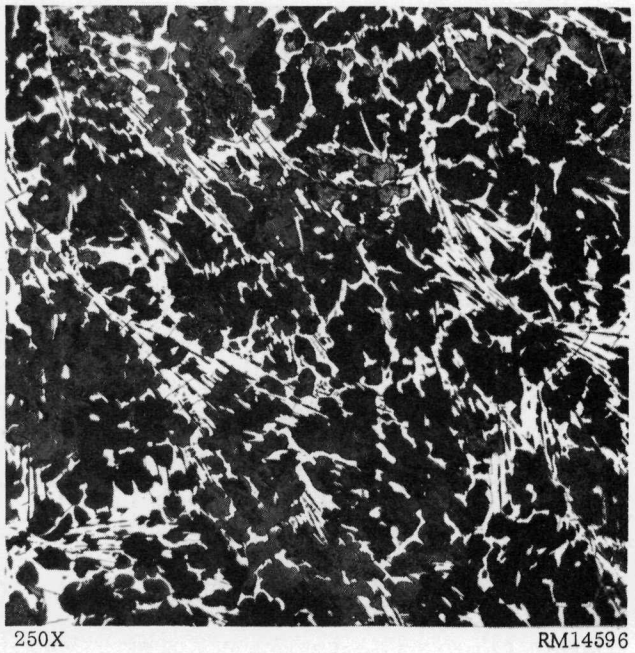

250X RM14596

a. Uranium Monocarbide-10 w/o Dimolybdenum Carbide

The dark phase is primary UC, the remainder is a dimolybdenum carbide-uranium monocarbide eutectic structure.

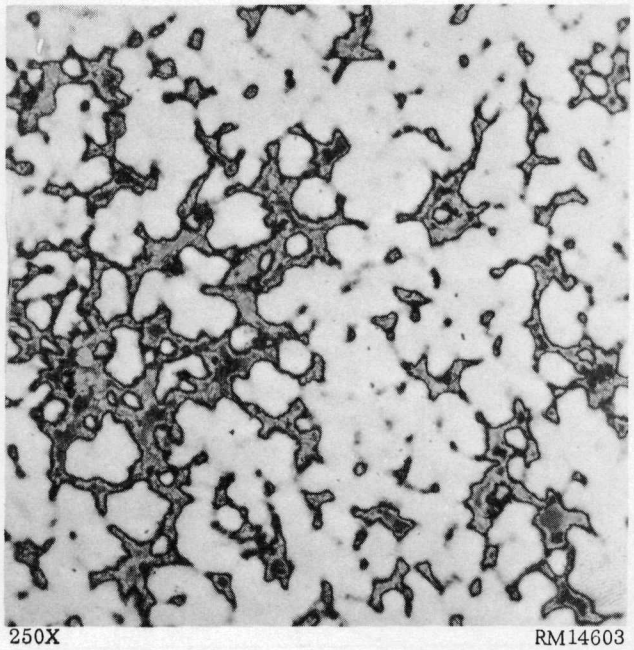

250X RM14603

b. Uranium Monocarbide-10 w/o Niobium Carbide

The white areas are probably rich in niobium.

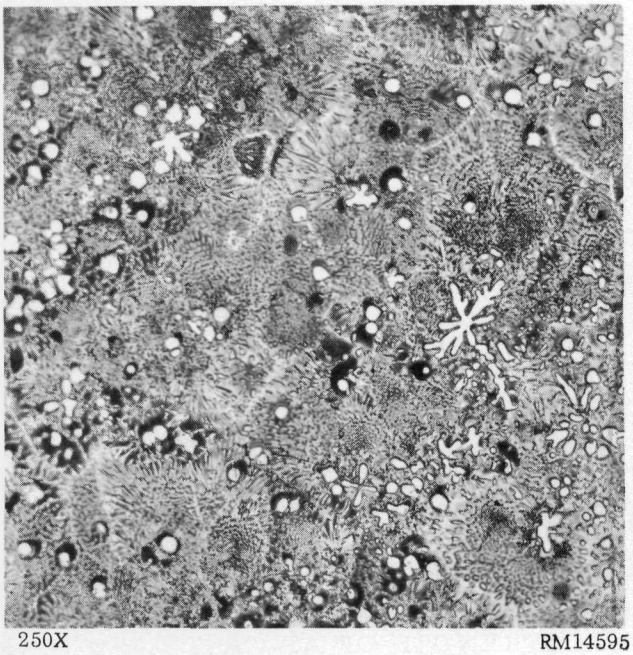

250X RM14595

c. Uranium Monocarbide-10 w/o Titanium Carbide

The white particles in this nearly eutectic structure are probably titanium carbide.

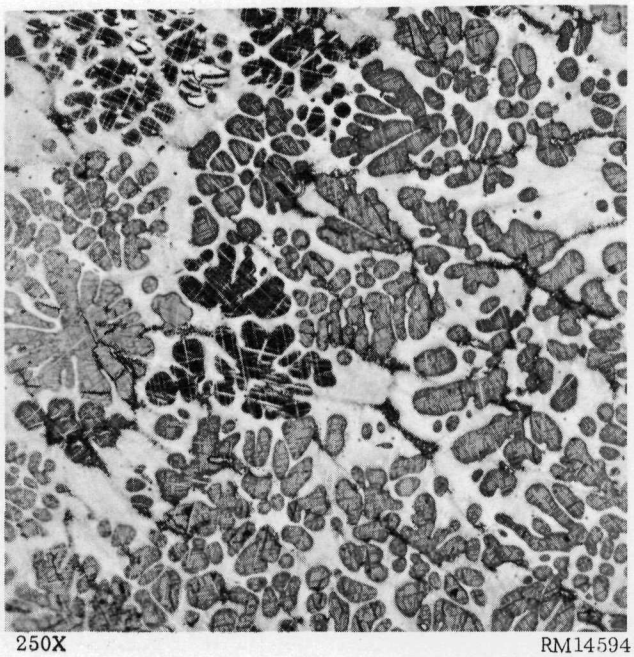

250X RM14594

d. Uranium Monocarbide-10 w/o Vanadium Carbide

The dark phase is UC, the white is probably an unresolved eutectic between UC and VC.

FIGURE 27. STRUCTURES OF URANIUM CARBIDES CONTAINING ADDITIONS THAT APPEAR PROMISING FOR IMPROVING CORROSION RESISTANCE

TABLE 11. PROPERTIES OF URANIUM MONOCARBIDE CONTAINING ADDITIONS OF NIOBIUM AND NIOBIUM CARBIDE

Nominal Alloy Content (Balance UC), w/o	Alloy Density, g per cm^3	Alloy Resistivity, microhm-cm	Transverse Rupture Strength, 1000 psi	Compressive Rupture Strength, 1000 psi	Weight Loss in 1 Week in Santowax R at 350 C, mg/(cm^2)(day)	Knoop Hardness, kg per mm^2
0.5 Nb	--	--	--	--	--	640
1 Nb	13.4	52	--	18.9	1.1	--
5 Nb	13.4	74	27.2	204.9	0.5	--
10 Nb	12.8	--	30.0	--	--	1150
20 Nb	12.7	94	--	--	--	--
1 NbC	13.3	52	9.6	27.0	0.7	680
2.5 NbC	13.0	76	--	--	--	--
5 NbC	12.6	98	10.9	24.9	1.1	1170
7.5 NbC	12.0	55	25.1	--	0.2	--
10 NbC	12.4	94	21.1	68.3	0.5	1320
15 NbC	12.4	106	25.1	--	0	--

Metallographic and X-ray diffraction examinations of these and the other alloys of uranium carbides allow the following tentative conclusions to be drawn with regard to the constitution of the ternary carbide systems:

(1) Chromium, iron, and nickel appear in castings of uranium monocarbide and uranium dicarbide as metals. The terminal solubilities of these phases in one another are negligible.

(2) The pseudobinary systems of uranium monocarbide and uranium dicarbide with the carbon-rich carbides of molybdenum, titanium, tungsten, and vanadium involve eutectics. The uranium monocarbide-dimolybdenum carbide eutectic is near 30 mole per cent dimolybdenum carbide; the uranium dicarbide-dimolybdenum carbide eutectic is near 1 mole per cent dimolybdenum carbide. Terminal solubilities of these carbides in one another are negligible. The uranium monocarbide-titanium carbide eutectic is near 30 mole per cent titanium carbide. The solubility of titanium carbide in uranium carbide is less than 2 mole per cent. The uranium dicarbide-titanium carbide eutectic is at uranium dicarbide. The solubilities of uranium dicarbide and titanium carbide in one another are negligible. The uranium dicarbide-tungsten carbide eutectic is near 30 mole per cent tungsten carbide. The solubilities of tungsten carbide and uranium dicarbide in one another are negligible. The uranium monocarbide-vanadium monocarbide eutectic is near 60 mole per cent vanadium carbide and at or below 1800 C. The solubility of vanadium carbide in uranium monocarbide is between 4 and 9 mole per cent vanadium carbide. The uranium dicarbide-vanadium monocarbide eutectic is near 50 mole per cent vanadium carbide. The solubility of vanadium carbide in uranium dicarbide is negligible. Titanium and tungsten metals apparently displace uranium from uranium monocarbide. However, countrary to the constitution diagrams presented in BMI-1441 (May 31, 1960)[12], uranium metal displaces vanadium and, probably, molybdenum from vanadium monocarbide, divanadium carbide, and dimolybdenum carbide.

(3) The pseudobinary systems of uranium monocarbide with niobium monocarbide, tantalum monocarbide, and zirconium carbide are solid solutions. The pseudobinary systems of uranium dicarbide with niobium monocarbide, tantalum monocarbide, and zirconium carbide are apparently eutectic-type systems with the eutectics near uranium dicarbide. The solubilities of these carbides in uranium dicarbide are much less than 10 mole per cent. Niobium, tantalum, and zirconium metals displace uranium from uranium monocarbide.

Future Work

Future work will include additional studies of the properties of binary uranium-carbon alloys with particular emphasis upon the mechanical and physical properties of the alloys at elevated temperatures. Depending upon the suitability of the testing techniques, one or more mechanical properties such as hardness, compressive strength, transverse bend strength, impact strength, or modulus will be determined as a function

of temperature to at least 900 C on binary alloys of uranium containing about 5, 7, and 9 w/o carbon. Physical properties such as specific heat, thermal-expansion coefficient, thermal conductivity, and resistivity will be determined as a function of temperature on these same alloys.

An attempt will be made to define some of the causes of the extreme variability in the strength and corrosion resistance of uranium carbides. These studies may entail investigations of residual stresses in castings, thermal-shock resistance, notch sensitivity, machining techniques, the effect of exposure to moist atmospheres, the effect of impurities, and the grain structure of castings.

Studies of the rate of formation of U_2C_3 in uranium-7 w/o carbon alloys and of the rate of decomposition of UC_2 in uranium-9 w/o carbon alloys will be continued. Property determinations will be made in conjunction with these studies in an attempt to define any problems that may arise as a result of these solid-state transformations during reactor operation.

Alloying and coating studies will be continued in a supporting effort directed toward overcoming the storage and corrosion problems associated with unalloyed uranium carbides. It is expected that efforts in the area of alloying will be directed primarily toward the elements having the lower neutron-capture cross sections, namely niobium and zirconium, but additions of molybdenum and vanadium may be used to introduce a refractory metallic constituent into the microstructure or to produce a low-melting intercarbide eutectic to improve castability.

A minor effort will also be made to evaluate the feasibility of improving the compatibility of uranium monocarbide with niobium and zirconium by introducing excess carbon in one form or another into the contact area.

DIFFUSION STUDIES OF URANIUM MONOCARBIDE

The rates of diffusion in uranium monocarbide are of interest in obtaining an understanding of mechanical and physical properties of this material at high temperatures and in understanding the structural nature of this material. Some of the processes which can be understood better when diffusion-rate data are available are environmental reactions, diffusion of fission products, precipitation phenomena, relaxation of stresses, and sintering. It is intended to obtain the rate of interdiffusion of uranium and carbon in uranium carbides, the rate of self-diffusion of uranium in uranium monocarbide, and the rate of self-diffusion of carbon in uranium monocarbide.

The interdiffusion rate of uranium and carbon in uranium carbides was determined by holding liquid uranium saturated with carbon at a constant temperature in a graphite crucible. The diffusion zone, consisting of layers of UC and UC_2, was measured metallographically after holding at temperatures ranging from 1600 to 2000 C. In order to obtain diffusion coefficients from the data, it was assumed that diffusion rates in the uranium monocarbide and uranium dicarbide layers are essentially the same. A more detailed discussion of the interdiffusion study can be found in BMI-1370 (August 1959).[14] The final results of this study are plotted in Figure 28. See also TID-7589 (April 1960).[13] The data for interdiffusion at temperatures of 1200, 1300, and 1400 C

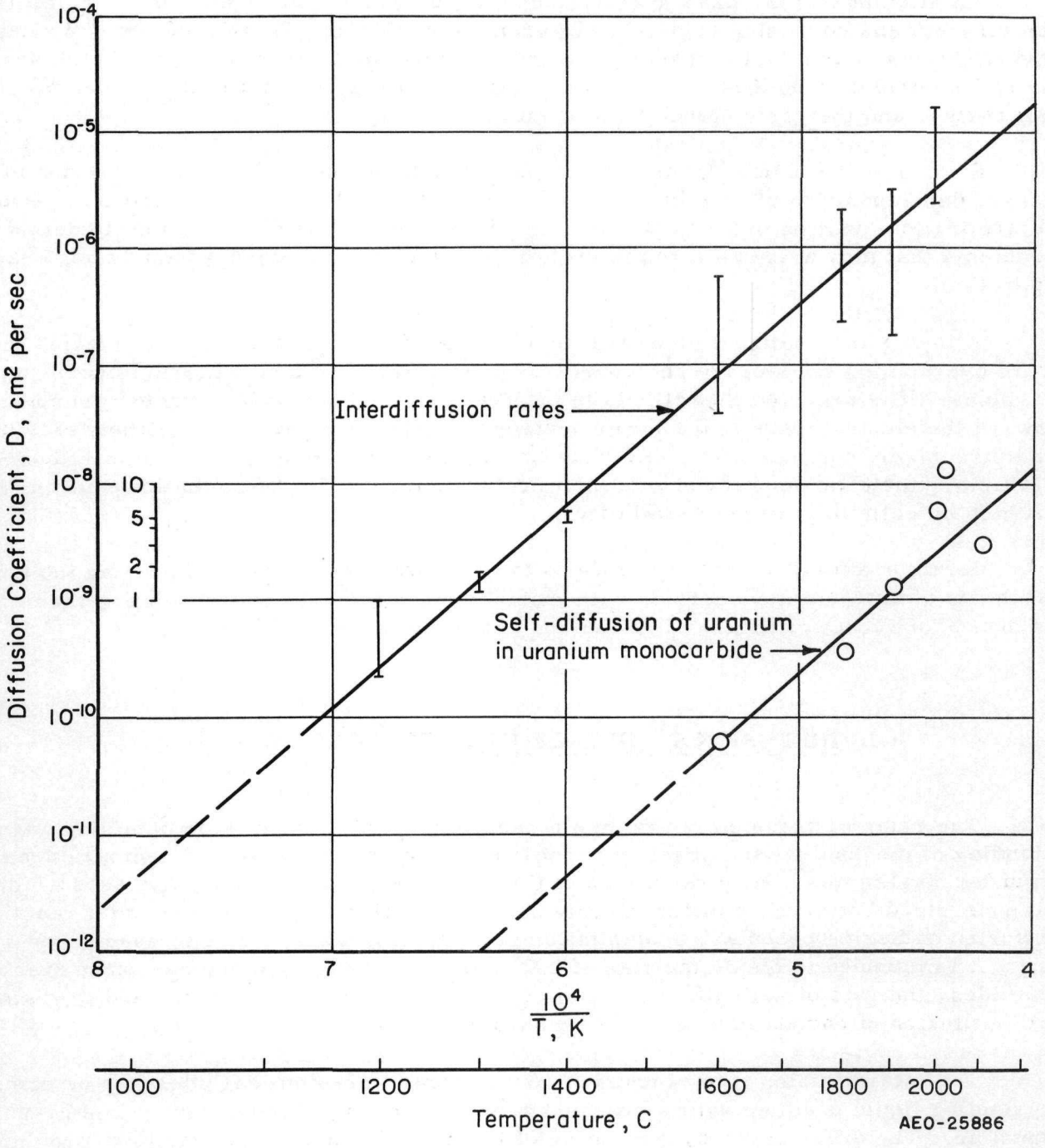

FIGURE 28. DIFFUSION RATES IN URANIUM CARBIDE

were obtained from the reaction-zone measurements of E. L. Swarts.[15] Diffusion coefficients were calculated from these measurements by the method described by W. Jost.[16] These interdiffusion data can be represented by the equation:

$$D = 148\, e^{\frac{-79,000}{RT}},$$

where

D = interdiffusion coefficient, cm^2 per sec

148 = diffusion constant, cm^2 per sec

79,000 = activation energy, cal per mole

R = universal gas constant, 2 cal/(mole)(C)

T = temperature, K.

Currently, the self-diffusion rate of uranium in uranium monocarbide is being studied using a tracer technique. The diffusion couple consists of a foil of enriched uranium metal sandwiched between two pieces of depleted uranium monocarbide rod. The uranium foil is 0.001 in. thick and contains 93.3 per cent uranium-235; the cast carbide rods are approximately 0.38 in. in diameter and 0.25 in. long, and the uranium used in making the carbide contains 0.04 per cent uranium-235. The carbon content of the carbide is 4.9 w/o carbon, which is slightly in excess of the stoichiometric amount found in uranium monocarbide. This excess is required to eliminate free uranium particles from the microstructure of the rods and to provide sufficient carbon for converting the uranium foil to monocarbide during the bonding operation.

The diffusion couples are wrapped in 0.001-in. tantalum foil and placed in an outgassed graphite bottle for bonding and annealing. The compressive force necessary for bonding is obtained by utilizing the difference in the thermal-expansion coefficients of graphite and uranium monocarbide. Bonding is accomplished by heating the assembly for 4 hr at 1400 C. The bonded couples are cooled to room temperature, inspected, and surface ground to remove any enriched uranium that may have flowed out of the bond line and down the side of the specimen. The specimens are then returned to the same bottle for annealing.

After annealing, the couples are inspected metallographically and autoradiographically. Samples for analysis are obtained by abrading the couple on the bottom of a flat aluminum dish containing a little 600-grit silicon carbide powder and a few milliliters of 0.1 normal nitric acid to dissolve the uranium monocarbide. The specimen is measured and weighed periodically so as to obtain samples in solution from layers 0.0005 in. thick. These samples are analyzed for uranium-235 content by counting the 0.184-Mev gamma ray emitted by uranium-235. The diffusion coefficient (D) is calculated using the equation[17]:

$$D = \frac{\ln(c_2/2) - \ln(c_1/2)}{X_2^2 - X_1^2} \cdot \frac{1}{4t},$$

where t is the time for diffusion in seconds, c is the enrichment, and X is the distance in centimeters between the center of the enriched foil and the center of the sample. The

results of these self-diffusion measurements are also shown in Figure 28 and can be represented by the equation:

$$D = 0.23\, e^{\frac{-82,000}{RT}},$$

where D is the diffusivity, R is the universal gas constant, T is the temperature in K, 0.23 is the diffusion constant in cm^2 per sec, and 82,000 is the activation energy in cal per mole.

It has been established that the crystal structure of uranium monocarbide is face-centered cubic. In this structure, each atom of uranium is surrounded by six atoms of carbon, and each atom of carbon is surrounded by six atoms of uranium, making the principal interatomic bonds all of the uranium-carbon variety. Thus, the mechanism and activation energy for diffusion of atoms in this system could conceivably be the same for uranium and carbon atoms. This could explain why the curves in Figure 28 are nearly parallel, since the activation energy for diffusion is directly related to the slope of these curves. In the face-centered-cubic structure of uranium monocarbide, the (111) planes are alternately carbon and uranium atoms. Consideration of this fact and the large differences in the sizes and weights of uranium and carbon atoms could explain the differences in the self-diffusion coefficient for uranium in the monocarbide and the interdiffusion coefficient for uranium and carbon in uranium carbides.

Future work will include the preparation and analysis of additional couples to more accurately establish the coefficient for the self-diffusion of uranium in uranium monocarbide. An attempt will also be made to find a suitable technique for measuring the rate of self-diffusion of carbon in uranium monocarbide.

MECHANISM OF IRRADIATION DAMAGE

A program has been undertaken to study the important mechanisms of damage occurring during high-temperature irradiation of uranium monocarbide. This program has been designed specifically to study any radiation-induced changes in the structural and physical properties of uranium monocarbide. The program includes the determination of lattice strain and structural effects in uranium monocarbide by X-ray diffraction and electrical-resistivity measurements. Microstructural effects of irradiation are to be examined by optical and electron microscopy. Density and dimensional changes are to be studied as a function of burnup.

To better understand the effects of radiation on the uranium-carbon system, the stability of essentially single-phase structures of uranium sesquicarbide (U_2C_3) and uranium dicarbide (UC_2) are to be investigated in these studies. Another object of this irradiation-effects program is to attempt to explain the disappearance of the UC_2 second phase originally present in UC specimens irradiated in an earlier program at high temperatures and burnups.[4,5]

Conditions of Irradiation Experiments

Irradiations of uranium-carbon fuel materials involve six capsules in the BRR. The first two of these capsules each contained six specimens of natural uranium-5.0 w/o

carbon alloy. These specimens were annealed for 1 hr at 3270 F to relieve casting stresses and were irradiated to target burnups of 0.01 and 0.03 a/o of the uranium at temperatures not in excess of 500 F. The remaining four capsules will contain combinations of three different uranium-carbon alloys made from 10 per cent enriched uranium. These alloys are uranium-5.0 w/o carbon, uranium-6.7 w/o carbon, and uranium-8.5 w/o carbon. These latter specimens are to be irradiated to target burnups ranging from 0.1 to 0.7 a/o of the uranium at temperatures of 400 to 1600 F. The uranium-6.7 w/o carbon and uranium-8.5 w/o carbon specimens in these capsules will all be heat treated prior to irradiation, whereas the uranium-5.0 w/o carbon specimens will be irradiated in both the as-cast and heat-treated conditions. The heat treatments for these specimens were determined on the basis of studies performed on similar alloys made of natural uranium. The heat treatment for the uranium-5.0 w/o carbon specimens will be 5 hr at 2642 F, primarily for the purpose of relieving casting stresses. The specimens of uranium-6.7 w/o carbon will be heat treated at 2552 F for 15 hr to transform the specimens to an equilibrium structure showing U_2C_3 with some residual UC present. The uranium-8.5 w/o carbon specimens also will be heat treated at 2552 F for 15 hr once again primarily to relieve casting stresses.

All irradiation specimens are 1/2 in. long by 1/4 in. in diameter and are immersed in NaK during irradiation to insure good heat-transfer conditions within the capsules. The capsules are made of stainless steel and are designed to permit sampling of any gases released from the specimens during irradiation. The capsules designed for the high-temperature experiments are equipped with thermocouples for measurement of temperatures. The component parts of the high-temperature capsules as well as the NaK used in them have been subjected to purification treatments to reduce oxygen contents.

Results of Completed Experiments

The irradiation of the first two capsules containing specimens of natural uranium-5.0 w/o carbon has been completed and the postirradiation examinations have been performed. These specimens were irradiated to calculated burnups of 0.01 and 0.03 a/o of the uranium and experienced temperatures of less than 500 F. In general, the appearance of these specimens indicated that they suffered no damage as a result of the irradiation. The changes in the dimensions of the specimens were found to be small and well within the limits of experimental error. A slight trend toward decreased density was noticeable. The only major change noted in any property was a considerable increase in the electrical resistivity, as shown in Table 12.

TABLE 12. EFFECT OF NEUTRON RADIATION ON URANIUM-5.0 w/o CARBON ALLOY AT TEMPERATURES BELOW 500 F

Nominal Uranium Burnup, a/o	Density Decrease, per cent	Electrical Resistivity, microhm-cm		Lattice Strain, per cent
		Before	After	
0.01	0.3 to 0.9	34	92	0.14
0.03	0.2 to 0.5	34	94	0.17

X-ray diffraction data were obtained on minus 325-mesh powder prepared by crushing one specimen from each capsule. Preparation of the powder was carried out remotely under an argon atmosphere. About 25 mg of sieved powder was mounted in a plastic holder with a 1/4-mil-thick Mylar window and transferred to a lead-shielded specimen support on an X-ray diffractometer having a monochromated detector.

The interplanar spacings, half breadth, and integral breadth of the UC X-ray diffraction reflections were measured. Analysis of the X-ray diffraction line breadths indicated that internal lattice strains were the main cause of line broadening for the specimen irradiated to the 0.01 a/o burnup and that both crystallite fragmentation and lattice strain contributed to the line broadening for the specimen irradiated to the 0.03 a/o burnup. The root-mean-square lattice strain was estimated to be 0.14 per cent for the 0.01 a/o burnup specimen and 0.17 per cent for the 0.03 a/o specimen.

Metallographic examinations of one specimen from each of the first two capsules failed to reveal any microstructural changes. The same structure of UC with needles of residual UC_2, characteristic of hyperstoichiometric UC, was observed both before and after irradiation.

Discussion of Initial Results

The results of the initial irradiation experiments permit only tentative comparisons of properties and lattice constants as a function of burnup. Since both capsules were irradiated at similar temperatures to only relatively low burnups, no great dimensional changes were expected. The only property that exhibited a considerable change during irradiation was the electrical resistivity. The change was almost a 200 per cent increase. Since the resistivity values do not show a hyperbolic increase with increasing irradiation, it is thought that either a saturation of displaced interstitial atoms and vacancies in the lattice was attained early in the irradiation, or that this effect upon resistivity was due to some variable other than irradiation. However, the crystal-lattice expansions for the high- and low-burnup specimens, calculated from X-ray diffraction data, also indicate saturation of the UC crystal structure. From the lattice-expansion data, the indicated concentration of interstitial atoms is estimated to be 0.14 a/o in the specimen subjected to 0.01 a/o burnup or about 30 times the number of fissions. For the specimen subjected to 0.03 a/o burnup, it is believed that the crystallite size was reduced, resulting in some relief of crystal strain during the irradiation.

Status of Irradiation Experiments in Progress

Examination of the natural uranium-5.0 w/o carbon alloys irradiated to 0.01 and 0.03 a/o burnup is nearing completion. The only remaining research to be performed on these specimens is an electron-microscopy study of the structure. This study is now in progress.

Work directed toward irradiation and examination of three types of 10 per cent enriched uranium-carbon alloys is also in progress. Specimens of uranium-5.0 w/o carbon, uranium-6.7 w/o carbon, and uranium-8.5 w/o carbon alloys have been prepared, and their physical properties have been measured. The necessary heat treatments previously discussed have been performed on these specimens. The encapsulation

of these specimens into the four remaining capsules is presently in progress, and their irradiation is scheduled to begin in the BRR late in 1960. Special purification treatments of both the capsule parts and the NaK to be used in them have been performed to reduce their oxygen contents. The irradiation time required to obtain the maximum burnup, 0.7 a/o of the uranium is expected to be approximately 27 weeks. The time required for the 0.1 a/o burnup will be about 12 weeks. The postirradiation examinations will be similar to those performed on the specimens of natural uranium. However, included in these examinations will be sampling and analyses of any fission gases released during irradiation. Also, specimens from each capsule will be analyzed to determine the exact burnups. The two capsules containing specimens to be irradiated to low burnups will probably be discharged from the BRR during December, 1960, and the postirradiation examinations will be performed in the Battelle Hot-Cell Facility during January, 1961. The irradiation periods required for the specimens of the two high-burnup capsules should be completed by April, 1961. The postirradiation examinations of these specimens will probably be performed in the Battelle Hot-Cell Facility during May, 1961.

DISCUSSION AND EVALUATION

These research efforts have demonstrated the technical feasibility of preparing uranium carbide powders by reacting uranium metal with methane; the technical feasibility of cold pressing and sintering carbide powders containing excess uranium to more than 90 per cent of theoretical density; the possibility of hot pressing carbide powders to about 100 per cent of theoretical density; and the technical feasibility of melting and casting of 100 per cent dense uranium carbide ingots of any size up to 5 kg and of any right-cylindrical shape. Since all of these techniques use uranium metal as a starting material, the uranium carbide produced will certainly be more expensive than crude uranium metal. It does not follow, however, that slugs or rods of cast uranium carbide will be more expensive per unit than wrought slugs or rods of uranium metal. Additional efforts are in progress to improve compositional control in the melting and casting process.

Determinations of the physical, mechanical, and chemical properties of uranium carbides have confirmed most of the expectations of the potential of uranium carbide as a reactor fuel. The strength, hardness, and thermal stability of uranium carbides have been demonstrated to be more than adequate for the purposes of a reactor fuel. Uranium carbides are adversely affected by exposure to moisture, but this problem can be circumvented by avoidance of moist atmospheres or by suitable alloying. Several promising alloys have been developed, and techniques for coating uranium carbides with thin, protective films appear to have sufficient promise to warrant further development. The ranges of temperature in which uranium carbides are compatible with typical reactor materials have been crudely defined, and, in some cases, it appears that compatibility problems may limit the usefulness of uranium carbides. Techniques for increasing the temperatures at which uranium carbides are compatible with metals have not been adequately tested. Although most of the high-temperature properties of uranium carbides remain to be determined, diffusion data obtained at temperatures up to 2100 C suggest that uranium carbides will show appreciable resistance to deformation under stresses at least to 2100 C, and that creep will be negligible at temperatures below 1100 C.

Preliminary studies of the mechanism of radiation damage in uranium monocarbide have proved the validity of the test methods and have indicated that damage to the

monocarbide crystal lattice occurs at very low burnups. The importance of this damage at low burnups and its relation to eventual failure of uranium carbide as a coherent structural body in a nuclear reactor have not yet been determined.

The results obtained to date continue to support the expectation that uranium monocarbide will prove to be one of the most (if not the most) economical fuels for nuclear reactors using nonaqueous and nonoxidizing coolants.

PLANS FOR FUTURE WORK

The third period (Phase III) of the Fuel-Cycle Development Program study for the development of uranium carbide as reactor fuel will entail additional research in only four of the five areas of interest. Actually, the major effort will be expended in only two of these four areas. The work planned in each of these areas during Phase III is as follows:

I. Development of Alternate Fabrication Techniques: No work is planned.

II. Melting and Casting: The skull-melting and -casting technique will be studied further in an effort to improve control over the composition of the product. Effects of melting and casting variables such as feed and melt compositions, superheat, pouring time, and mold size and shape upon casting quality will also be investigated. Large specimens suitable for physical-property tests will be prepared.

III. Mechanical and Physical Properties: Studies of the mechanical and physical properties of binary uranium-carbon alloys will emphasize the determination of properties as a function of temperature. Alloys of uranium containing approximately 5, 7, and 9 w/o carbon will be examined for strength, thermal conductivity, thermal-expansion coefficient, resistivity, and, possibly, specific heat as a function of temperature from room temperature to about 900 C. Supporting efforts on binary uranium-carbon alloys will include studies of the effect of environmental conditions upon the properties of uranium carbides, studies of the effect of heat treatment upon the stability and properties of uranium carbides, and attempts to find a suitable technique for applying thin, metallic coatings to uranium carbide.

Studies related to improving the properties of uranium carbides by alloying with a third element will continue with particular emphasis upon achieving corrosion resistance and resistance to change during ordinary processing procedures.

IV. Diffusion Studies of Uranium Monocarbide: The rates of interdiffusion of uranium and carbon in uranium carbide have been defined from about 1200 to 2000 C. Studies of the rates of self-diffusion of uranium in uranium monocarbide in the temperature range from 1600 to 2100 C are nearing completion. These studies will be completed, and an attempt will be made to devise a method by which the self-diffusion rates of

carbon in uranium monocarbide can be measured. If a method can be found to make these measurements, they will be made.

V. Mechanism of Irradiation Damage in Uranium Monocarbide: Two capsules containing natural uranium monocarbide have been irradiated to burnups of 0.01 and 0.03 a/o of the uranium contained in them. Examinations of the irradiated specimens are essentially complete. Four additional capsules have been prepared containing specimens of enriched uranium alloyed with 5.0, 6.7, and 8.5 w/o carbon and subjected to various heat treatments. These will be irradiated at various temperatures up to 1600 F (approximately 900 C) and to various burnups ranging up to 0.7 a/o of the uranium. The irradiated specimens will be examined for any changes in dimensions, density, resistivity, microstructure, and lattice strain. The incremental burnups are intended to provide specimens which may disclose the mechanism of damage to the carbide crystal structure. The variations in composition are intended to show any gross differences in thermal or radiation stability as a function of composition. The heat treatments are intended to produce stable and stress-free structures in certain specimens prior to irradiation. The effects of reactor irradiation can then be compared with respect to both types of specimens. The samples irradiated at different temperatures may or may not show different rates of lattice strain and structural damage because of different rates of diffusion of lattice defects as a function of temperature.

REPORTS ISSUED UNDER THIS PROGRAM

(1) Rough, F. A., Chubb, W., "Progress on the Development of Uranium Carbide-Type Fuels, Phase I Report on AEC Fuel-Cycle Program", BMI-1370 (August 21, 1959).

(2) "Progress in Carbide Fuels, Notes from the Second AEC Uranium Carbide Meeting Held at Battelle Memorial Institute, March 22, and 23, 1960", TID-7589 (April 20, 1960).

(3) Rough, F. A., Chubb, W., "An Evaluation of Data on Nuclear Carbides", BMI-1441 (May 31, 1960).

REFERENCES

(1) Secrest, A. C., Foster, E. L., and Dickerson, R. F., "Preparation and Properties of Uranium Monocarbide Castings", BMI-1309 (January 2, 1959).

(2) Rough, F. A., and Dickerson, R. F., "Uranium Monocarbide – Fuel of the Future?", Nucleonics, 18, 74-77 (March, 1960).

(3) Phillips, W. M., Chubb, W., and Foster, E. L., "Direct Casting of Uranium Monocarbide Reactor Fuel Elements", to be published.

(4) Rough, F. A., Hare, A. W., Price, R. B., and Alfant, S., "Irradiation of Uranium Monocarbide", Nuclear Sci. and Eng., 7, 111-121 (February, 1960).

(5) Hare, A. W., and Rough, F. A., "Irradiation Effects on Massive Uranium Monocarbide", BMI-1452 (July, 1960).

(6) Dayton, R. W., and Tipton, C. R., Jr., "Progress Relating to Civilian Applications During July 1960", BMI-1455 (August 1, 1960).

(7) Tripler, A. B., Synder, N. J., and Duckworth, W. H., "Further Studies of Sintered Refractory Uranium Compounds", pp 38-44, "Estimated Thermodynamic Values" (J. J. Ward), BMI-1313 (January 27, 1959).

(8) Rossini, F. E., "Selected Values of Physical and Thermodynamic Properties of Hydrocarbons", American Petroleum Institute (1953).

(9) Evans, U. R., Metallic Corrosion Passivity and Protection, 2nd Ed., Edward Arnold & Co., London (1946) p 137.

(10) Egloff, G., The Reactions of Pure Hydrocarbons, Reinhold Publishing Co., New York (1937) p 46.

(11) Dayton, R. W., and Tipton, C. R., Jr., "Progress Relating to Civilian Applications During May, 1960", BMI-1442 (Rev.) (July 12, 1960).

(12) Rough, F. A., and Chubb, W., "An Evaluation of Data on Nuclear Carbides", BMI-1441 (May 31, 1960).

(13) "Progress in Carbide Fuels, Notes from the Second AEC Uranium Carbide Meeting Held at Battelle Memorial Institute, March 22, and 23, 1960", TID-7589, (April 20, 1960).

(14) Rough, F. A., and Chubb, W., "Progress on the Development of Uranium Carbide-Type Fuels, Phase I Report on AEC Fuel-Cycle Program", BMI-1370 (August 21, 1959).

(15) Swarts, E. L., "The Action of Molten Uranium on Graphite", Trans. AIME, 215, 553-54 (August, 1959).

(16) Jost, W., Diffusion in Solids, Liquids, and Gases, Academic Press, New York (1952), pp 74-75.

(17) Jost, W., loc. cit., pp 258-59.

FAR:WC/nb